NBS

Field Performance of Three Residential Heat Pumps in the Heating Mode

James Y. Kao
William J. Mulroy
David A. Didion

U.S. DEPARTMENT OF COMMERCE
National Bureau of Standards
National Engineering Laboratory
Center for Building Technology
Building Environment Division
Gaithersburg, Maryland 20899

February 1987

Sponsored by:
of Building Energy Research and Development
Department of Energy
ngton, DC 20585

NBSIR 87-3528

FIELD PERFORMANCE OF THREE RESIDENTIAL HEAT PUMPS IN THE HEATING MODE

James Y. Kao
William J. Mulroy
David A. Didion

U.S. DEPARTMENT OF COMMERCE
National Bureau of Standards
National Engineering Laboratory
Center for Building Technology
Building Environment Division
Gaithersburg, Maryland 20899

February 1987

Sponsored by:
Office of Building Energy Research and Development
U.S. Department of Energy
Washington, DC 20585

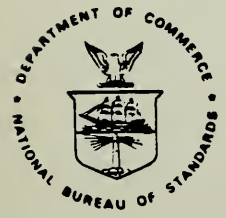

U.S. DEPARTMENT OF COMMERCE, Malcolm Baldrige, *Secretary*
NATIONAL BUREAU OF STANDARDS, Ernest Ambler, *Director*

ABSTRACT

This report presents the results of a field performance study of three heat pumps operating in the heating mode. The objective of this study was to evaluate the thermal, energy, defrosting, cycling, and other related performance under in-situ conditions and to confirm the validity of Department of Energy (DoE) test procedures by comparing these field results with those obtained in the laboratories. The seasonal COPs without auxiliary heat were 1.83, 2.31, and 1.92. The seasonal COPs with auxiliary heat were 1.71, 1.95, and 1.60. General agreement was found in two houses for cycling rates and building load estimation. Defrost penalty was found to be light above 40°F. One house was analyzed for cyclic performances. The cyclic degradation factor (C_D) was found to be worse than the optional factor (0.25) of the DoE procedure.

Key Words: Defrosting; field performance; field performance of heat pumps; heat pumps; heat pump test methods; heating seasonal performance

ACKNOWLEDGEMENTS

This study was sponsored by the U.S. Department of Energy, Office of Building Energy Research and Development. The authors wish to express their appreciation to Charles W. Hurley for his assistance in gathering technical information during this study.

TABLE OF CONTENTS

LIST OF TABLES

LIST OF FIGURES

SI CONVERSION FACTORS

MULTIPLY	BY	TO OBTAIN
Btu	1.055	kJ
Btu/h	0.293	W
Btu/min	0.0488	W
°F	°C = (°F - 32)/1.8	
ft^2	0.0929	m2
ft^3/min, cfm	0.472	L/S
inch	25.4	mm
inch of water	249	Pa
ton of refrigeration	3.52	kW

1. INTRODUCTION

During 1980 and 1981, the National Bureau of Standards (NBS) instrumented and collected data from three air-source, residential heat pumps to evaluate the field performance of these units. The three heat pumps were already in operation and were selected from the homes of volunteers of NBS employees in the Washington, D.C. area. Microprocessor-based data acqusition systems were used to gather and reduce the energy, weather and other related information. A previous report describes the selection criteria of the house/heat-pump sets, the instrumentation details, the hardware and software of the data acqusition systems, and the preliminary data reduction procedures [1].

Test procedures for heat pumps were issued by the United States Department of Energy (DoE) in 1979 [2] and require heat pump manufacturers to perform certain laboratory tests to determine the heat pump's thermal and energy performance. These test procedures were based on research results performed earlier at NBS [3,4]. A heat pump of the same model as one of the three field units was subsequently tested in accordance with the DoE procedures.

The purposes of this field studyare two-fold:

(1) To give a comprehensive evaluation of the thermal, energy, defrosting, cycling, and related performance of heat pumps operating under in-situ conditions; and

(2) To compare the results of the field performance with those obtained previously in the laboratory and, thus, to verify the heat pump test procedures.

The analysis of the cooling data obtained in the 1980 cooling season for the three field units was published in a previous report [5]. In this report the field performance of these heat pumps for the 1980-1981 heating season is analyzed and presented.

2. HOUSE AND HEAT PUMP SYSTEM DESCRIPTION

The heat pumps monitored in this study were split systems. A brief description of the three houses and some elements which may affect the heating performance of the heat pumps are shown in table 2.1.

Table 2.1 House and Heat Pump Description

Item	HOUSE 1	HOUSE 2	HOUSE 3
1 House style	1 story	1 story	1 1/2 story
2 House wall construction	brick	frame	frame
3 Approx. living area, sq. ft	2900	1800	1600 (1000 s.f. bsmt unused)
4 Occupancy during working hours	vacant	occupied	vacant
5 System nominal cool. capacity	2 1/2 tons	3 tons	3 tons
6 HP expansion device	non-bleed exp. valve	constant area device	constant area device
7 Auxiliary heater	15 kW electric	15 kW electric	15 kW electric
8 Defrost initiation	diff. air pressure across outdoor coil reaches 0.5 in. of water	timer (90 min of comp. on-time) and temp. in outdoor coil reaches 27°F	diff. air pressure across outdoor coil reaches setting for 12 seconds and refrig. temp. in outdoor coil reaches 39°F
9 During defrost	in cooling mode and outdoor fan off	in cooling mode, outdoor fan off, and one aux. heater on	in cooling mode, outdoor fan off, and one aux. heater on
10 Defrost termination	outdoor refrig. temp. reaches 65°F	outdoor coil temp. reaches 80°F or defrost for 10 minutes	outdoor refrig. temp. reaches 75°F or reaches 45°F for 5 minutes
11 Fins per inch of outdoor coil	14	17	13

3. FIELD DATA ACQUISITION SYSTEM

3.1 System Description

The field data acquisition system and instrumentation of the heat pumps are described in detail in the previous reports [1,5]. An on-line microcomputer at each field site performed the following functions: (1) controlling of the data monitoring strategy; (2) processing of data obtained from the various analog and digital points to engineering units; (3) performing computations for preliminary data reduction; and (4) recording the results on magnetic disks for further processing. The disks in the field were replaced as necessary. Each time a disk was replaced, the operation of the system was manually checked. The sensors and instrumentation were calibrated periodically. A central microcomputer located in the NBS laboratory was used to further process the field disks for data analysis. This Z-80 based central computer had 64K static memory and two disk drives.

3.2 Measurements and Instrumentation

Twelve analog and digital input points plus two on/off mode conditions were measured and recorded at each field location. A schematic illustration of the measured data locations is given in figure 3.1. The measured and recorded quantities, and the sensing element types are listed in table 3.1. A complete description of the signal conditioning, computer interface system, and the preliminary data reduction equations is given in reference 1.

Table 3.1 Description of Field Data Points

	Measured Quantity and Units	Symbol	Sensing Element (or Calculated)	Scan	Data Acquisition [1] Cyclic	Daily	Half Hour
1	Pitot tube differential pressure (inches H_2O)	DP	Pitot tube with variable capacitance ΔP cell	IV[2]			
2	Return air dew point temp. (F)	TDPR	LiCl/RTD dew point cell	IV	CTIA	CTIA	IV
3	Outdoor air dew point temp. (F)	TDPO	LiCl/RTD dew point cell	IV		HSA	
4	Barometric pressure (inches H_2O)	PATM	Pressure cell with diaphragm potentiometer	IV			IV
5	Return air dry bulb temp. (F)	TRET	Linear thermistor	IV	CTIA	CTIA	IV
6	Outdoor air dry bulb temp. (F)	TOUT	Linear thermistor	IV	EOC	HSA	IV
7	Differential temp. across indoor coil	DT	Type-T thermocouple	IV			IV
8	Supply air dry bulb temp. (F)	TSUP	Linear thermistor	IV			IV
9	Compressor and outdoor fan energy (pulse)	DIG1	Watt-hour meter with magnetic latch pulse initiator	RT			RT
10	Indoor fan and 1st stage heater energy (pulse)	DIG2	Watt-hour meter with magnetic latch pulse initiator		CIT		RT
11	2nd stage heater energy (pulse)	DIG3	Watt-hour meter with magnetic latch pulse initiator		CIT		RT
12	Condensate metering pump (pulse)	DIG4	Positive displacement solenoid metering pump with optical coupler				RT
13	Compressor ON-OFF	MODE 0-ON	Opto-coupler	IV			IV
14	Outdoor Fan ON-OFF	MODE 3-OFF	Opto-coupler	IV			IV
15	Compressor on time for a cycle (sec)	CTIM	Clock card		CIT	CIT	
16	Defrost time for cycle (sec)	DTIM	Clock card		CIT	CIT	
17	Volumetric flow rate in return duct (ft^3/min)	FLOW	Calculated	IV			IV
18	Sensible heat (Btu)	QS	Calculated	TI	CIT	DIT	
19	Latent Heat (Btu)	QL	Calculated		CIT	DIT	
20	Compressor, outdoor fan and c.c. heater energy (Wh)	ECMP	Calculated		CIT	DIT	
21	Indoor fan energy (Wh)	EFAN	Calculated		CIT	DIT	
22	Auxiliary heaters (Wh)	EHET	Calculated		CIT	DIT	
23	Coefficient of performance	COP	Calculated		CIT	DIT	

[1] Refer to text

[2]
IV: instantaneous value
CIT: cycle integrated total
CTIA: compressor time integrated average
DIT: daily integrated total
EOC: end-of-cycle value
HSA: average of the 48 half hour scans for the day
RT: running total for a cycle
TI: value for the last time increment

3.3 Data Format and Scanning Requirements

During the data collection, a cycle was defined as either a heating plus an off period, or a heating plus a defrost period. The data acquisition software was designed to record four types of data format:

(1) Scan data. Data recorded, among others, were the instantaneous scans of the indoor and the outdoor temperatures, the sensible heat output of the indoor coil between consecutive scans, the accumulated heat output of the indoor coil, and the accumulated energy input to the outdoor unit. The accumulated data were the totals from the start of each heating cycle. There were no auxiliary heat data in these files. High data acquisition rates were desirable at the beginning of the on-cycle and during the defrost. These data were recorded at intervals of 10 seconds for the first 2 minutes, 30 seconds for the next 4 minutes, 60 seconds for the next 6 minutes, and 5 minutes until the compressor stopped or defrost started. These data were used subsequently to calculate and record the integrated cycle data. Since they occupied a great deal of storage space, the scan data were recorded every eleventh cycle.

(2) Cycle data. Data included, among others for each cycle, were the heat output of the indoor coil, the energy input of the outdoor unit, the energy input of the indoor fan, the energy input of the auxiliary heaters, the total compressor run-time (including defrost), and the defrost time. Also recorded were the indoor and the outdoor temperature averaged over the cycles.

(3) Daily data. Data were accumulated or averaged for each day and recorded on the disks at midnight.

(4) Half-hour data. Instantaneous readings of certain data at every half hour were recorded on the disks.

Thirteen data items, measured and computed, were recorded for each of the above four types of data format. These thirteen items together with the day and time of the moment of recording, and the status of the heat pump (in heating, defrosting, off, or malfunction) formed a "record". These "records" were used for further reduction and analysis of the heat pump performance.

4. FIELD TEST RESULTS OF THREE UNITS

Table 4.1 summarizes the test results of the three heat pumps. Although the heating data collection period was about half a year (line 2), the data available for analysis covered 3828, 2427, and 3278 hours (line 6) for the three units which indicated that about 25.5%, 40.2%, and 26.6% of the time (line 7) data were lost or useless, or the systems were turned off. Since the available data are not distributed equally during the data gathering period for the three units, caution should be exercised in comparing the performances of the units.

In data analysis, data stored under "cycle" data file for all three units were used to calculate the cyclic heat output, cyclic energy input, cycling rate, cyclic coefficient of performance (COP), heating seasonal performance, and the defrost characteristics. Since calculation for steady state performance required only certain segments of the cycles, data stored under "scan" data file were used to compute the steady state performance, the part load factor (PLF), heating load factor (HLF), and the degradation factor (C_D). Steady state and associate performance were analyzed for unit 3 only.

Figure 4.1 shows the capacity variations of a typical compressor on-cycle. The outdoor temperature during this particular cycle was about 33°F and the unit required frequent defrosting. The negative capacity at the beginning of the cycle indicated that this cycle started right after a defrost period. The capacity increased rapidly until it reached a peak in about 6 to 8 minutes

Table 4.1 Comparison of Three Field Units

ITEM		UNIT 1	UNIT 2	UNIT 3
1	Nominal cooling capacity, refrig.tons	2 1/2	3	3
2	Heating season data collection period	10/3/80-5/4/81 (5136 h)	10/3/80-3/20/81 (4056 h)	11/16/80-5/20/81 (4464 h)
3	No. of total cycles	4428	3692	3737
4	Total compressor-on time, hour	1427	1450	1923
5	Avg. compressor-on time per cycle, min/cycle	19.3	23.6	30.9
6	Total cycle time avail.for analysis, hour	3828	2427	3278
7	Percent of time data not avail., %	25.5	40.2	26.6
8	Avg. cycle time, minute	51.9	39.4	52.6
9	avg. percent compressor-on in a cycle, %	37.3	59.9	58.7
10	No. of defrost cycles	141	916	465
11	Total defrost time, hours	4.82	65.10	32.09
12	Avg. defrost time per defrost cycle, min	2.05	4.26	4.14
13	Defrost time/ compressor-on time, %	0.34	4.49	1.67
14	Tot.seasonal output, incl. aux. heat, Btu x 10^6	30.536	47.608	54.279
15	Tot.seasonal output, excl. aux. heat, Btu x 10^6	27.898	40.897	42.665
16	Percent of aux. heat used during season, %	8.6	14.1	21.4
17	Avg. heat output, excl.aux.heat, Btu/h	19550	28200	22190
18	Avg.heat output/ cycle, excl.aux.heat, Btu/cycle	6300	11080	11420
19	Avg. heating load, Btu/h	7980	19620	16560
20	Seasonal COP without aux. heat	1.83	2.31	1.92
21	Seasonal COP with aux. heat	1.71	1.95	1.60
22	Max. cycle rate, cph	2.31	2.95	2.74

and started to decrease gradually after about 20 minutes due to frost formation on the outdoor coil. The system then started the defrost at about 44 minutes from the beginning of the cycle. During the defrost period, the capacity dropped to negative values even with some auxiliary heat on. This particular defrost lasted for almost 5 minutes. Figure 4.2 is the corresponding chart of the energy input to the outdoor unit. After the initial surge, the energy input was quite constant during the entire heating cycle. A decrease of less than 3% was recorded when ice was formed on the outdoor coil. Then the energy input dropped sharply and stayed low during the first 2 minutes of the defrost because of the switching of the refrigerant path and the stopping of the outdoor fan. Finally, the power input surged to a level even higher than that measured during the heating cycle. This was caused by the loss of condensing capacity and the high discharge pressure of the system which helped to finish the cycle.

4.1 "Cycle" Data Analysis

4.1.1 Indoor and Outdoor Conditions

The three houses were equipped with electro-mechanical wall thermostats. Thus, the indoor temperature and the system cycling patterns were strongly influenced by the anticipator settings of these thermostats. The average indoor temperatures over the entire heating season, based on the available data and as measured by the sensors located in the return air ducts, were 70.7°F, 70.2°F, and 69.5°F, respectively for the three units. Figure 4.3 shows the temperature distribution of the average

indoor air with respect to 5°F temperature bins of the outdoor temperature. All three houses generally had higher indoor temperature when the weather was warm. The indoor temperature dropped at various rates when the outdoor became cooler. These curves demonstrate clearly the droop characterisics of the room thermostats. The exceptions were the 7°F bin and the 57°F or 62°F bin of unit 2 and the 7 to 22°F bins of unit 3 where the trend was reversed. These exceptions were probably caused by manual resetting of the thermostats by the occupants. The total indoor temperature differences caused by thermostat droop and manual reset were approximately 9°F, 11°F, and 2°F for the three houses respectively for the entire heating season.

Figure 4.4 shows the outdoor temperature distribution of the three houses. Data were derived from the available good data periods, excluding weather records when the heat pump monitoring systems were receiving bad data. Because of the house location difference and the time difference of available data, considerable variations appear in the figure.

4.1.2 Defrost

Figures 4.5 to 4.7 depict both absolute defrost time and percentage of compressor run-time of defrost in terms of outside air temperature bins. Unit 1 (figure 4.5) had its highest defrost time in the 30-35°F bin and it defrosted in all temperature bins below 37°F (Data were not available for the 5°F-10°F bin). The pattern of defrost time was not clearly shown except that most defrost was done between the outside temperature of 25°F to 40°F.

Unit 2 (figure 4.6) also had the highest defrost time in the 30-35°F bin. It decreased toward the 5°F-10°F and 50°F-55°F bin. As a percentage of compressor run-time, the defrost occurred more (8 to 9%) in the 5°F-15°F bins than the other bins. Therefore, the effect of defrost was more important for the low outdoor temperature range than for the overall heating season. Unit 3 (figure 4.7) had about the same defrost pattern as Unit 2 except that Unit 3 did not have any defrost above 40°F. The large amount of low temperature defrosting done by Unit 3 was not expected since this unit had a demand defrost initiation system whereas Unit 2 used only a simple timer to initiate defrost (see table 2.1). The conclusion to be drawn from this is that all demand defrost systems are not equally effective in avoiding unnecessary defrosts. The shape of the Unit 2 timer-initiated defrost is reasonable. Below the balance point the unit will run continuously resulting in a constant number of defrost initiations. Defrost time for each defrost cycle will be high at high temperatures because of the need to melt frost, and at low temperatures because of the lower temperature of the mass of the coil with respect to the termination temperature. These test results differ from the assumption of the heat pump test procedures which assume that defrost is negligible below 17°F of outdoor temperature and is occurring up to 45°F.

There were large differences in the total defrost time between the three units. This can be seen from lines 10, 11, and 12 in table 4.1, and figures 4.8 and 4.9. The total defrost time for

the heating season were 4.82, 65.10, and 32.09 hours, respectively for the three units. Even considering the unequal distribution of the available data, as mentioned previously, the difference of the ratios of defrost time to total compressor run-time is significant. The three units had 0.34, 4.49, and 1.67% of defrost time over compressor run-time. Unit 1 had a simple demand defrost initiation criteria and did not initiate defrost as often as the other two units (see table 2.1). A timer in unit 2 made defrost available after every 90 minutes of compressor run-time (together with temperature sensing of outdoor coil temperature). Evidently this arrangement enabled this unit to go on defrost more often than the other two units. The number of defrost cycles during the heating season were 141, 916, and 465, respectively for the three units. Figures 4.8 and 4.9 show comparisons of the defrost time by outside temperature bins of the three units in absolute time and percentage of compressor run-time. Unit 2 had higher fin density (thus less space between fins) on the outdoor coil than the other two units (table 2.1). Presumably it would require more frequent defrost. However, these units were not instrumented to yield data for more detailed study on the process of frost and defrost.

4.1.3 Heating Load and Unit Sizing

The cyclic records of total energy output delivered to the houses and the compressor on and off time were used to derive the building load. The building load profiles of the three houses are shown in figure 4.10. They had a generally linear relationship to the outdoor temperature, except for the coldest

bins of units 2 and 3. This is consistent with what was shown in figure 4.3 and discussed in paragraph 4.1, i.e., the indoor temperature of units 2 and 3 were manually reset upward during the cold period. The slope of these lines, of course, were basically reflections of the house characteristics, such as the thermal insulation, construction, house geometrics, and internal loads. The linear regression equations for the building loads as functions of outdoor temperature bins are:

$$Y = 22.85 - 0.3569\ X \quad \text{for house 1,}$$

$$Y = 48.67 - 0.7934\ X \quad \text{for house 2, and}$$

$$Y = 56.40 - 1.015\ X \quad \text{for house 3.}$$

The DoE procedure assumes heating load to be zero at outside temperature of 65°F. The above three equations yield zero building loads when outside temperature are 64.0°F, 61.3°F, and 55.6°F, respectively for the three houses.

Figures 4.11 to 4.13 show the heat output at various temperature bins during the heating season. The lower portions of the stacked bars are for the heat output without auxiliary heat and the top portions are for the auxiliary heat only. The numbers above the bars are the percentage of auxiliary heat used in that bin. Figures 4.14 to 4.16 show the heat output without auxiliary heat, the auxiliary heat, and the total of these two in percentage of the yearly total. Some conclusions may be drawn from these charts:

(1) Manual thermostat reset may be seen for all three units during the entire heating season. When a thermostat was adjusted

upward during the heating season and the amount of adjustment was over the differential of the first stage (for the compressor) of the thermostat, the auxiliary heater would respond even when the weather was warm (the balance points of these units will be discussed later). This can be seen for all three units. Unit 1 had considerable amount of auxiliary heat use even above the 37°F outdoor temperature bin (figures 4.11 and 4.14). Units 2 and 3 had very high auxiliary heat use at low outdoor temperature. Since these data were derived from the "cycle" data file, it is impossible to determine the causes of the auxiliary heat--by the thermostat adjustment or by the load demand.

(2) Sizing of heat pumps are usually determined by matching the peak cooling load of a building and the cooling capacity of a heat pump system. The deficiency of the heating capacity of the heat pump is made up by the auxiliary heaters. These charts show that the heat output from the auxiliary heat for unit 1 during the cold bins was relatively smaller than those for units 2 and 3. Excluding the 7°F bin for unit 2 and the 7 through 22°F bins for unit 3, where the manual thermostat resetting was quite evident, units 2 and 3 used larger portion of auxiliary heat during the rest of the cold season. That indicates that unit 1 was more adequately sized than units 2 and 3 in relation to the heating load of the houses.

(3) The DoE rating procedure assumes that a heat pump be sized according to the following equations:

$$\text{minimum design heating requirement} = \begin{cases} \dot{Q}_{ss}(47)\,\dfrac{(65 - T_{OD})}{60}, & \text{for regions I, II, III, IV, and VI} \\ \dot{Q}_{ss}(47), & \text{for region V} \end{cases}$$

and

$$\text{maximum design heating requirement} = \begin{cases} 2\,\dot{Q}_{ss}(47)\,\dfrac{(65 - T_{OD})}{60}, & \text{for regions I, II, III, and IV} \\ 2.2\,\dot{Q}_{ss}(47), & \text{for region V} \end{cases}$$

where $\dot{Q}_{ss}(47)$ is the steady state capacity at 47°F and T_{OD} is the outdoor design temperature for the DoE region. The test houses were located in DoE region IV which had a T_{OD} of 5°F. The actual winter design temperature for the area in which the test homes were located was around 10°F. The DoE assumed design heating requirements (DHR) at T_{OD} are compared to the actual design heating requirements (figure 4.10) at the local design temperature in table 4.2.

Table 4.2 Comparison of DoE and Field Design Heating Requirements

	DoE minimum DHR, kBtu/h	DoE maximum DHR, kBtu/h	Field DHR, kBtu/h
Unit 1	32.1 #	64.2	19.3 ##
Unit 2	36.2 #	72.4	40.7 ##
Unit 3	32.4 ###	64.8	46.3 ##
Average	33.6	67.1	35.4

\# From a laboratory test [6].
\## From building load regression equations given previously.
\### From field test, see paragraph 4.2.1.

The field data indicate that the design heating requirements of Units 2 and 3 fall within the anticipated range of the DoE procedure. Unit 1 was oversized beyond the expectations of the procedure. The sizing, and selection of this unit was done by the home owner who was particularly concerned with energy conservation. Unit 2 was 12% above the DoE minimum DHR and Unit 3 was close to the midway between the minimum and maximum DoE DHRs. The single heating seasonal performance factor (HSPF) number used for Air Conditioning and Refrigeration Institute (ARI) listing and general advertising is that calculated at the minimum DHR for region IV. This data suggests that because of consumer concern with energy conservation it may be desirable for manufacturers to provide HSPF listings 50% below the DoE maximum DHR. For the same reason, the choice of the minimum DHR for advertising purposes appears reasonable as it is the average of this limited sample.

(4) The balance point of units 2 and 3 was somewhere between 37°F and 42°F bins when the auxiliary heat consumption changed markedly. No conclusion may be made about unit 1 because of the thermostat resetting.

4.1.4 Cyclic Coefficient of Performance

The "cycle" data were used to calculate the cyclic COP of the units at all outdoor temperature bins. Figures 4.17 to 4.19 show the cyclic COP of these units for the entire heating season. The right-most columns are the seasonal COP and the other columns are for the individual temperature bins. Both COP, with auxiliary heat and without auxiliary heat, are shown side by side. The

seasonal COP's without auxiliary heat were 1.83, 2.31, and 1.92 respectively for the three units. When the auxiliary heat was added, they dropped down to 1.71, 1.95, and 1.60. The balance points can also be estimated from these figures. Above the balance points, the COP of the two (with and without auxiliary heat) should be equal. Below these points, the COP of the period without auxiliary heat should be higher than that with electric heat. The result of unit 1 (figure 4.17) is again confused by the thermostat resetting. Unit 2 (figure 4.18) indicates a balance point of just above 42.5°F and unit 3 (figure 4.19) shows somewhere between 37°F and 42°F bins. The seasonal COP ratios (without and with electric heat) were 1.07, 1.18, and 1.20 for the three units. These numbers may also be interpreted to give a similar conclusion as stated in paragraph 4.3, that the heating capacity of unit 1 was larger than those of the other two units in relation to the house heating load. In fact, when comparing units 1 and 3, a higher COP of unit 3 (1.83 for unit 1 vs. 1.92 for unit 3) was reduced to a lower one (1.71 for unit 1 vs. 1.60 for unit 3) when auxiliary heat was also counted. These figures also show the cycling and the thermodynamic effects on the heat pump performance. When the outdoor temperature was above the balance point, the cycling dominated the performance. Below the balance point, the lower outdoor temperature caused the heat pumps to perform poorly.

4.1.5 Thermostat Cycling Rate

The heat pump cycling patterns are shown in figures 4.20 to 4.22. The data points shown in these figures are the average cycling

rates of the cycles falling within the 1/10 load ranges and the numbers below the data points are the number of cycles in that range. These data were derived from "cycle" data file after the elimination of defrost cycles and cycles where the thermostat settings were manually adjusted upward. Since defrost caused the systems to reverse the process regardless of the thermostatic status, all the defrost cycles were excluded in the cycling analysis. When a thermostat was adjusted manually upward, it always shortened the off-period of the same cycle causing the cycle to fall in the last (on-time/total cycle time=0.9 to 1.0) fractional on-time bin. It also caused the next on-period to be extraordinarily long with notably higher return air temperature and large auxiliary heat consumption. By examining all the cycles in the last fractional on-time bins and applying these criteria, these cycles were eliminated.

The peak cycling rates, N_{max}, were 2.31, 2.95, and 2.74 cycles per hour for the three units. These cycling rates are in agreement with the patterns of the indoor air temperature discussed in paragraph 4.1 and shown in figure 4.3 where the temperature droop of unit 1 is smaller than the other two units. The peak cycling rates of units 2 and 3 (2.95 and 2.74), occurred at approximately 50% of the heating load, are very close to the cycling-rate requirement of approximately 3 cycles per hour specified in the DoE heat pump test procedures. These figures also show the parabolic curves of the thermostat model developed in the cooling mode study [5]. The equation of the model is:

$$N = 4 N_{max} G (1-G)$$

where N is the cycling rate, N_{max} is the cycling rate at 50 percent on-time, and G is the fractional on-time corresponding to N. The values of the cycling rates in the .4 to .5 fractional on-time bins were used to plot the curves. These figures show that the model and the test data follow closely.

4.1.6 Heating Capacity of Defrost Cycles

The DoE test procedures require a "frost accumulation test" to determine the heating performance of a heat pump between two defrost periods and is used to indicate the effect of defrost on the heat pump performance. Briefly, the test requires that the performance of a complete cycle be recorded from the termination of a defrost cycle to the next automatically terminated defrost cycle. The results of the frost test is combined with those of the steady-state tests to establish the heat pump's capacity curve for estimating the heating seasonal performance factor (HSPF) and seasonal operation cost. Since the steady-state performance can only be derived from the "scan" file (will be discussed in section 4.2) and the "scan" file had only a very limited number of defrost cycles, "cycle" file data were used in this investigation to analyze the defrost cycle performance of unit 3.

For the field study, all defrost cycles (a cycle having a defrost period) which were preceded by defrost cycles were extracted from the file and analyzed. Figures 4.23, 4.24, and 4.25 show the

heating capacity, the power input, and the COP of these cycles. The total number of such cycles were 330 and the numbers shown below the data points in figure 4.23 were such cycles in the 5°F outdoor temperature bins. The regression lines in these three figures were weighted by these cycles and they will be discussed further in section 4.2.4.

4.2 "Scan" Data Analysis

As stated previously, the "cycle" file gives only the summed-up data of the cycles, it can not be used to extract information requiring only segments of cycles. Therefore, the "scan" file was used to investigate the steady-state performance. The steady-state results were then combined with the cyclic results of the same cycles to calculate the heating load factors and other part load performance (discussed later). This was analyzed for unit 3 only.

Representative cycles at different outdoor temperatures of unit 3 were examined and it was found that the heat output reached steady-state conditions at about 6 to 8 minutes after the cycles were started. However, it took less than a minute for the power input to reach steady-state. Although over 3700 cycles were recorded in the "cycle" file for this unit, some cycles were not available for analysis because either the "cycle" or the "scan" file of the same cycles contained bad data. Many cycles during mild weather were also eliminated, because they never reached steady-state conditions. The total number of cycles analyzed for steady-state performance were 204.

4.2.1 Steady-State Performance

The heat output, power input, and COP of heat pump 3 are plotted against the outdoor temperature in figures 4.26, 4.27 and 4.28. The equations of the regression lines are:

$Y = 205 + 7.11\ X$ for heat output,

$Y = 153 + 1.42\ X$ for power input, and

$Y = 1.57 + 0.0190\ X$ for COP.

These equations are used to calculate the capacity and COP at 47°F and 17°F. Table 4.3 compares these results with those obtained in laboratory tests on an identical unit [6].

Table 4.3 Comparison of Field and Laboratory Test Results

	Field results	Lab test	Difference
Capacity at 47°F, Btu/h	32350	36200	+ 11.9%
COP at 47°F	2.46	2.79	+ 4.9%
Capacity at 17°F, Btu/h	19550	20510	+ 4.9%
COP at 17°F	1.89	1.92	+ 1.2%

It should be noted that the field data contained all cycles, including defrost cycles, whereas the laboratory tests under the DoE test procedure had relatively clean outdoor coils. The DoE tests require a defrost cycle preceding the tests and the minimum duration of the test to be half an hour. The frosting and defrosting action of the field unit may have contributed to the lower capacity and the COP.

Taking this into account would reduce the discrepancy at 17°F but would not explain the performance difference above the defrosting regime at 47°F. One possible cause for such observed data would

be a lower refrigerant charge in the field test unit. This would reduce performance at high temperatures where superheat would occur in the evaporator but would have little effect at low temperatures where the unit would be flooding through the evaporator and storing excess refrigerant in the accumulator.

4.2.2 Part Load Performance

Heating load factor (HLF) is defined [2] by the equation

$$HLF = \frac{Q_{cyc}}{Q_{ss}},$$

where the quantity Q_{cyc} is the heating done for an entire cycle, including an on-period and a subsequent off-period and Q_{ss} is the amount of heating that would have been done for the entire cycle at the steady-state output rate. It is an indication of the combined effect of the building load and the capacity of the heat pump system at a given time of the season. Figure 4.29 is a plot of the fractional on-time against the HLF. The deviations of the values between the HLF and the 45 degree line represent the loss caused by cycling. The degree of frosting on the outdoor coil resulted in much scattering between the fractional on-time of 0.6 and 0.85 (all cycles having defrost were deleted in fractional on-time analysis, since their fractional on-time is always one). When the data points below 42°F outdoor temperature are eliminated as shown in figure 4.30, the scattering of the rest of the data is much reduced. The data also show that below the outdoor temperature of 42°F all cycles had fractional on-time above 0.6. The DoE test procedure requires the frosting effect to

be neglected above 45°F.

The cyclic performance test of the DoE procedures specify that the test be performed at 47°F outdoor temperature and at a 20% building load (6 minutes on and 24 minutes off). By fitting all data points above 45°F (numbered 30) with a straight line, the equation is

$$Y = -0.080 + 0.939\ X.$$

At 0.2 fractional on-time the HLF is 0.108. This HLF value and the corresponding value of part load factor (PLF) will be used later to compare the cyclic degradation factor.

Part load factor is defined [2] as:

$$PLF = \frac{COP_{cyc}}{COP_{ss}}.$$

The part load factor represents the COP change effected by part load cycling of the unit. The PLF and the fractional on-time relationship is shown in figure 4.31. The regression line equation is

$$Y = 0.663 + 0.332\ X\ .$$

At a fractional on-time of 0.2, the PLF is 0.729.

Figure 4.32 plots HLF against PLF. This figure gives the cyclic effect taking account of off-cycle and cycle starting losses. Therefore it is the loss caused by the cycling alone and is called the cyclic degradation factor, C_D. Its equation form is [2]:

$$C_D = \frac{1-PLF}{1-HLF}$$

Using this equation and the previously derived values of HLF (0.108) and PLF (0.729), C_D is calculated to be 0.304. The laboratory test value for the cyclic degradation factor was 0.375 [7]. For comparison to field data this laboratory measured C_D should be multiplied by the ratio of field maximum cycling rate, N_{max} = 2.74, to that of the laboratory test, N_{max} = 3, giving C_D = 0.342 (see appendix A). The DoE test procedures allow the heat pump manufacturers the option of assuming a C_D of 0.25 in calculating a heat pump's seasonal performance. The cyclic degradation factor may be expressed on the HLF vs PLF figure by a straight line having the slope of C_D. The area above this line represents the cyclic inefficiency. In figure 4.32 three lines are shown for the C_Ds of field result (0.304), laboratory test (0.342), and the DoE option (0.25). For this particular house and heat pump, the DoE optional degradation factor is more lenient than degradation factors found from both laboratory test and field measurements.

4.2.3 Thermostat Cycling Rate

The cycling rates of the 187 cycles are shown in figure 4.33. These points do not include the cycles having defrost, as was explained before. Averaging the cycling rates of the data points between .48 and .52 fractional on-time yielded a maximum cycling rate, N_{max}, of 2.75 which is very close to 2.74 as derived from all cycles of the "cycle" file (paragraph 4.1.5).

4.2.4 Seasonal Capacity Profile

As stated previously in section 4.1.6, the DoE procedure combines the steady-state capacity with the frost accumulation capacity to give the heat pump's seasonal capacity profile. To construct a similar profile from the field data, figures 4.23, 4.24, and 4.25 of the defrost cycles and figures 4.26, 4.27, and 4.28 of the steady-state data may be used. The power input of the defrost cycles were very close to the steady-state cases (Y = 150 +1.41 X in figure 4.24 vs Y = 153 + 1.42 X in figure 4.27). Yet, the capacity of the defrost cycles was much lower than the steady-state capacity at lower outdoor temperature (Y = 98 + 9.04 X in figure 4.23 vs Y = 205 + 7.11 X in figure 4.26). The slope of the defrost cycles is steeper than that of the steady-state line. This is contrary to the DoE assumption that between 17°F and 45°F the slope of the capacity curve is relatively flat. Figure 4.34 shows the capacity profiles. The broken line is constructed by using DoE procedure and laboratory test data points.

Using the laboratory test results in accordance with the DoE procedures and the building load data of 36000 Btu/h (at 17.5 F) obtained from the field for unit 3 (figure 4.10), the calculated heating seasonal performance factor (HSPF) is 1.89. Using the total energy output and input for the entire heating season of unit 3 from the field, the HSPF was 1.60. The DoE test procedure yields a +18.1% difference. A substantial portion of the increased performance indicated by the DoE procedure is the result of the higher value measured in the laboratory at the 47°F steady state rating point. Performance under steady state

operation should be substantially the same in both laboratory and field and it is therefore suspected that the field unit may have had its performance reduced by some problems such as undercharging. Discounting this the DoE procedure would still have predicted high for this unit because of the high defrost penalty it exhibited.

5. DISCUSSION AND CONCLUSION

Field data were collected and the heating performance of three heat pump units evaluated. Two major types of data were collected and used to evaluate the cyclic performance parameters and seasonal performance. The first type consisted of scan data collected at various intervals during the on portion of a cycle. The second type consisted of cycle data in which data were averaged or summed, as appropriate, for an entire on-off cycle. Cycle data were collected for every cycle throughout the test period.

Cycle data were analyzed for all three heat pumps. The conclusions drawn from cycle data analysis were:

* The parabolic thermostat profile assumed by the DoE test procedure was confirmed. This profile was also confirmed by the cooling mode tests analyzed in [5] where derivation of the parabolic thermostat model is also presented.

* The DoE test procedure assumes a maximum cycling rate at 50% run time of 3 cph. The test units had maximum cycling rates of 2.31, 2.95, and 2.74 cph. Unit 1 (2.31 cph) was felt to be nontypical because of thermostat setpoint changeS by the occupants, hence the assumption of 3 cph for the maximum cycling rate is validated as typical for heating mode operation. The maximum cycling rates in the cooling mode (1.64, 2.13, and 2.28 cph) were considerably lower [5].

* The degree day bases for the three houses were 64.0°F, 61.3°F, and 55.6°F (average 60.3°F) suggesting that the traditional degree day base of 65°F which is used in the DoE rating procedure may be somewhat high, particularly in view of trends toward better insulation, reduced infiltration, and heavier use of indoor appliances in modern homes.

* On average the units were sized to meet the DoE minimum design heating requirement confirming use of this point for single point listing and advertising purposes.

* One unit was sized for the house heating load substantially below the DoE minimum design heating requirement as a result of energy conservation concerns on the part of the owner. It may be desirable, to promote energy conservation, for manufacturers to extend their HSPF tables to reflect lower minimum design heating requirements.

* The DoE procedure assumes a substantial defrost penalty up to 45°F. The field tested units did not show a substantial penalty over 40°F.

* The DoE procedure assumes that the defrost penalty reduces to 0 at 17°F as result of the air holding little humidity. This was substantially true for unit 1 which had demand defrost. On the other hand the defrost penalty stayed approximately constant for unit 2 which had timer (90 minute interval) initiated defrost. This is reasonable since a substantial amount of energy is necessary to warm the metal mass of a coil up to the cutoff

temperature for an unnecessary, timer initiated defrost. Surprisingly, unit 3 which had demand defrost behaved in much the same way as unit 2 but at a lower energy consumption level indicating overly easy defrost initiation. The current DoE test procedure seems to characterize demand defrost best. As an improvement, either a penalty could be subtracted from timed defrost units or the length of the 17°F test period extended to allow the inclusion of defrost penalty at this rating point. Neither of these suggested solutions would account for the possibility of wind initiation of overly sensitive demand defrost systems.

Scan data were only analyzed for unit 3. These were used primarily to analyze cyclic performance. A unit identical in make and model to this unit was tested in the NBS laboratories and the laboratory results are compared to the field test results with the following conclusions:

* The cyclic degradation factor, C_D, used to characterize unit cyclic performance includes an assumption about thermostat performance. A derivation is presented in Appendix A to show that C_D is proportional to the maximum cycling rate, N_{max}, which occurs at 50% on time. Hence for comparison between laboratory and field results the cyclic degradation factor should be multiplied by the ratio of the respective N_{max} values. Analysis of the cooling mode data reported in [5] on this unit confirms this point. The laboratory measured value of 0.36 is multiplied by an N_{max} ratio of 1.64 cph to 3 cph. Therefore, the field

measured C_D of 0.18 compares closely to the adjusted laboratory measured value of 0.20.

* The cyclic test procedure of measuring C_D was validated for heating mode operation by comparing laboratory tests to the field results. The field measured C_D was 0.304. The laboratory measured value after adjusting for cycling rates was 0.342.

* The DoE test procedure allows use of a default value of 0.25 for CD in lieu of a tested value. Both the field (C_D = 0.30) and laboratory (C_D = 0.38 before adjusting and 0.34 after adjusting) results indicating that the manufacturer would be likely to use the default instead of the test values for rating calculations. This was also true for the laboratory measured cooling C_D (0.36).

* The C_D approach to cyclic loss calculation is based upon the assumption that the part load factor, PLF, is a linear function of the heating load factor, HLF, when the HLF is greater than 0.2. This was verified by presentation of a plot of PLF vs HLF based on field test data. Characterization of this curve for HLF less than 0.2 is difficult because of insufficient data. It would be expected to have a shape similar to those of the cooling mode curves as shown in [5] which decrease rapidly below cooling load factor of 0.2 and pass through the point 0,0 because of off-cycle parasitic losses (control circuit and crankcase heater powers).

6. REFERENCES

1. Hurley, C.W., Kelly, G.E., and Kopetka, P.A., "Using Microcomputers to Monitor the Field Performance of Residential Heat Pumps," National Bureau of Standards, NBSIR 81-2285 (June 1981).

2. Federal Register, Part III, Department of Energy,Office of Conservation and Solar Energy, Test Procedures for Central Air Conditioners, Including Heat Pump, Thursday, December 27, 1979.

3. Kelly, G.E., and Parken, W.H., "Method of Testing, Rating and Estimating the Seasonal Performance of Central Air-Conditioners and Heat Pumps Operating in the Cooling Mood," National Bureau of Standards, NBSIR 77-1271 (April 1978).

4. Parken, W.H., Kelly, G.E., and Didion, D.A., "Method of Testing, Rating and Estimating the Heating Seasonal Performance of Heat Pumps," National Bureau of Standards, NBSIR 80-2002 (April 1980).

5. Parken, W.H., Didion, D.A., Wojciechowski, P.H., and Chern, L., "Field Performance of Three Residential Heat Pumps in the Cooling Mode," National Bureau of Standards, NBSIR 85-3107 (March 1985).

6. Mulroy, W.J., and Didion, D.A., "The Performance of a Conventional Residential Sized Heat Pump Operating with a Non-Azeotropic Binary Refrigerant Mixture," National Bureau of Standards, NBSIR 86-3422 (October 1986).

7. Mulroy, W.J., "The Effect of Short Cycling and Fan Delay on the Efficiency of a Modified Residential Heat Pump," ASHRAE Transactions, v.92, pt. 1, American Society of Heating Refrigerating and Air-Conditioning Engineers, Inc. (1986).

7. APPENDIX A. Cyclic Degradation Factor

The cyclic degradation factor, C_D, can be derived from the parabolic model for thermostat performance and the effective time constant method for characterizing unit performance.

The parabolic thermostat model [5] assumes that the heating load factor is equal to the fractional on-time. This model predicts the length of an on-cycle as:

$$t_{on} = \frac{1}{4\ N_{max}\ (1 - HLF)} \qquad (1)$$

where t_{on} = length of on-cycle, h
N_{max} = cycling rate at CLF = 0.5, cph
HLF = heating load factor.

The effective time constant approach to characterizing unit capacity represents loss of unit efficiency as a short amount of running time at the steady-state power level but with no capacity. That is:

$$PLF = \frac{t_{on} - t_e}{ton} \qquad (2)$$

where PLF = part load factor
t_{on} = length of on-cycle, h
t_e = effective time constant, h

Substituting (1) into (2) gives:

$$PLF = (1 - 4\ N_{max}\ t_e) + (4\ N_{max}\ t_e)\ HLF$$

The slope of the HLF vs PLF line is C_D, hence:

$$C_D = 4\ N_{max}\ t_e$$

If a unit is tested at a cycling condition consistant with one value of N_{max} and is then operated in the field by a thermostat providing a different value for N_{max} the field value of C_D would be related to the laboratory value by the N_{max} ratio.

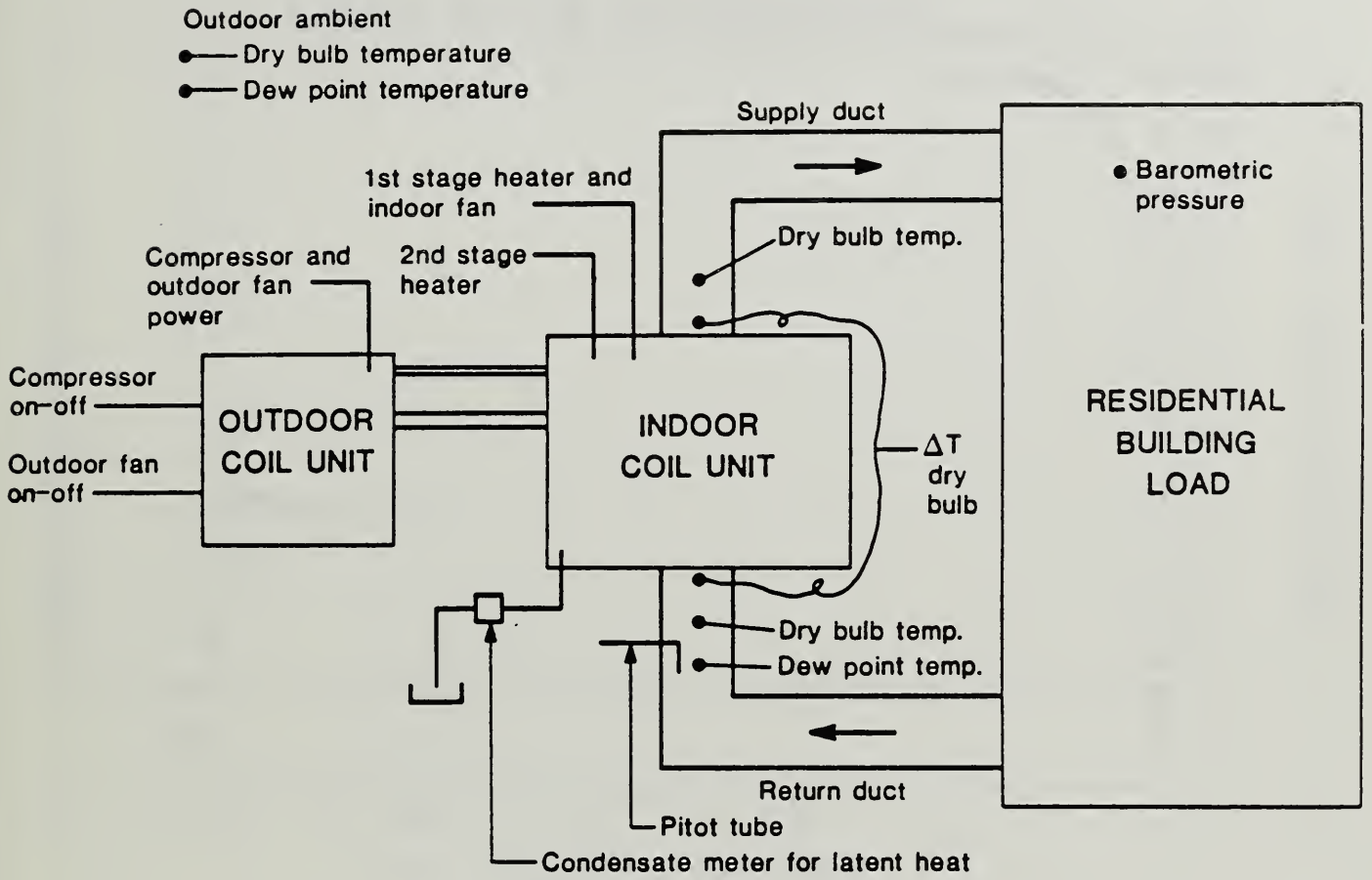

Figure 3.1 Schematic of Instrumentation for Typical Field Unit Showing Location of 12 Sensing Elements

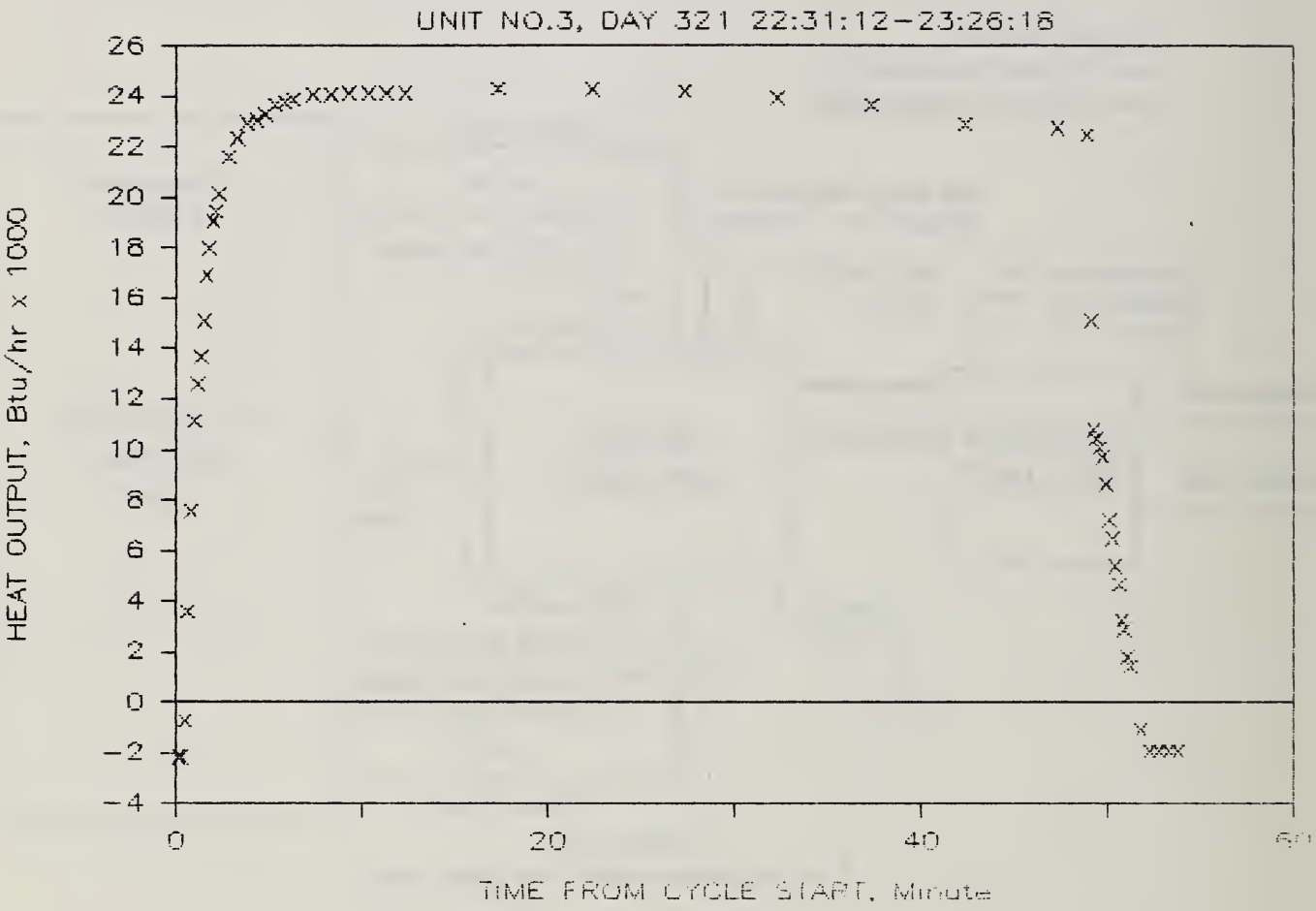

Figure 4.1 Heat Output of a Typical Cycle

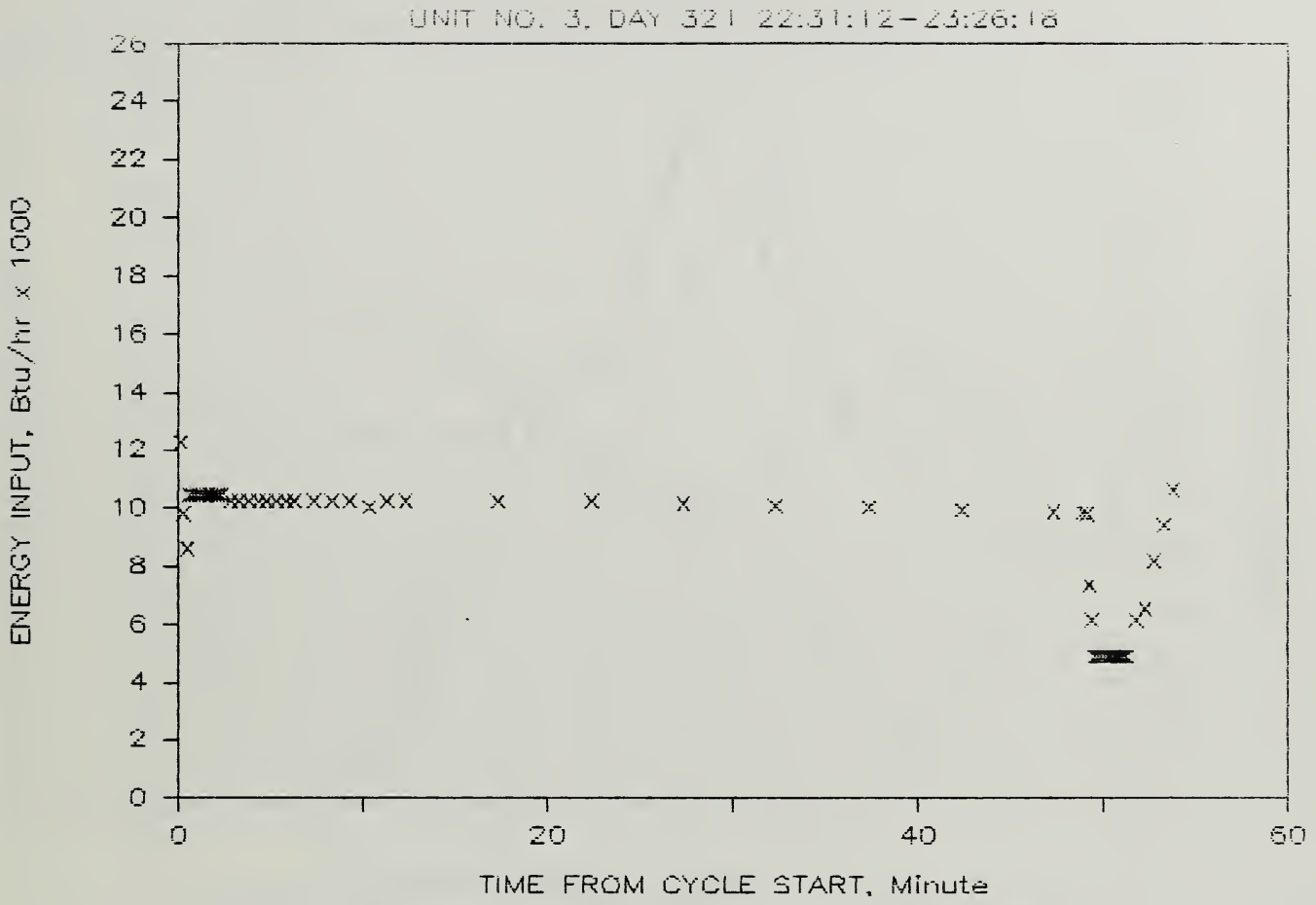

Figure 4.2 Energy Input to Outdoor Unit of a Typical Cycle

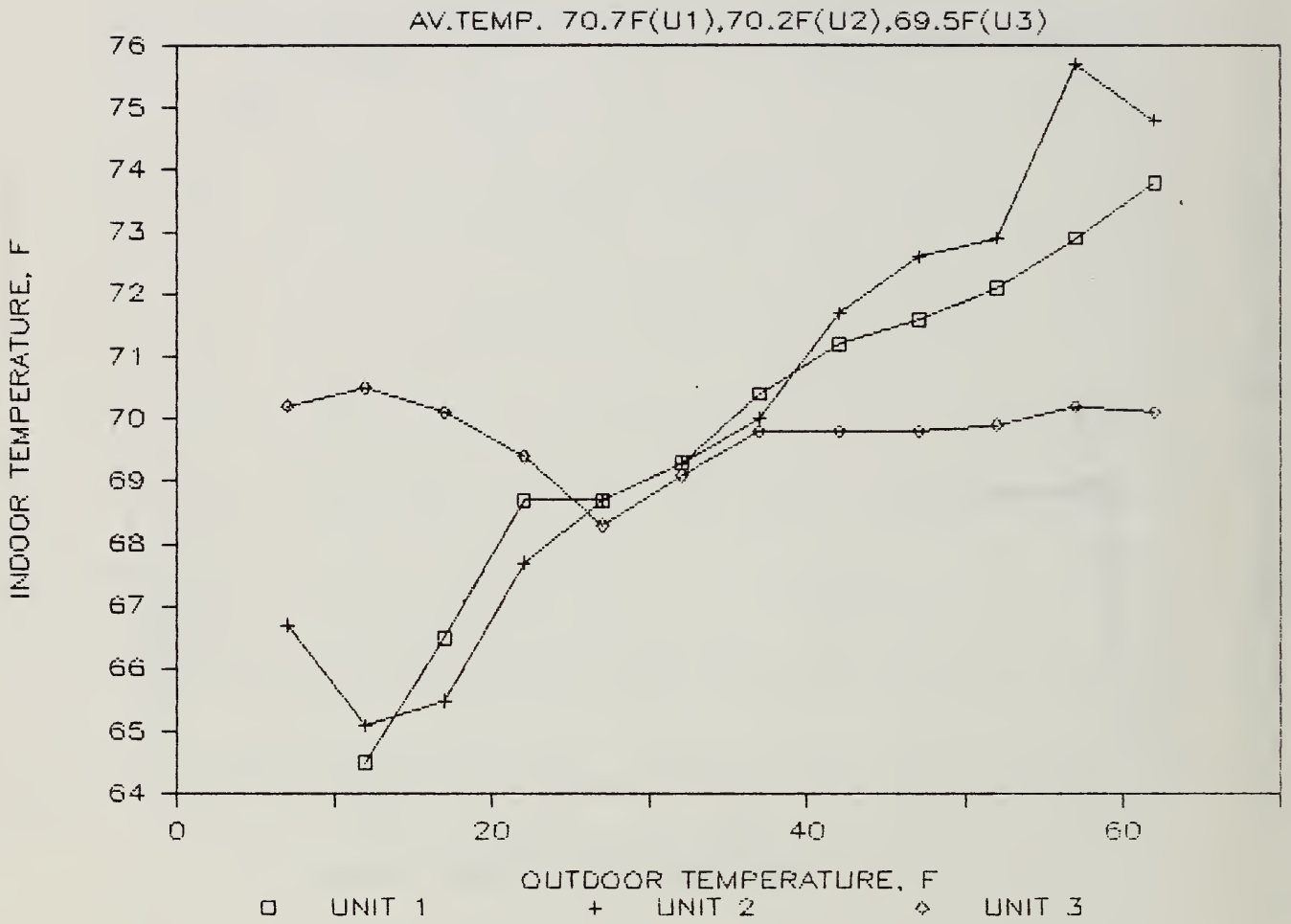

Figure 4.3 Outdoor Temperature vs. Indoor Temperature

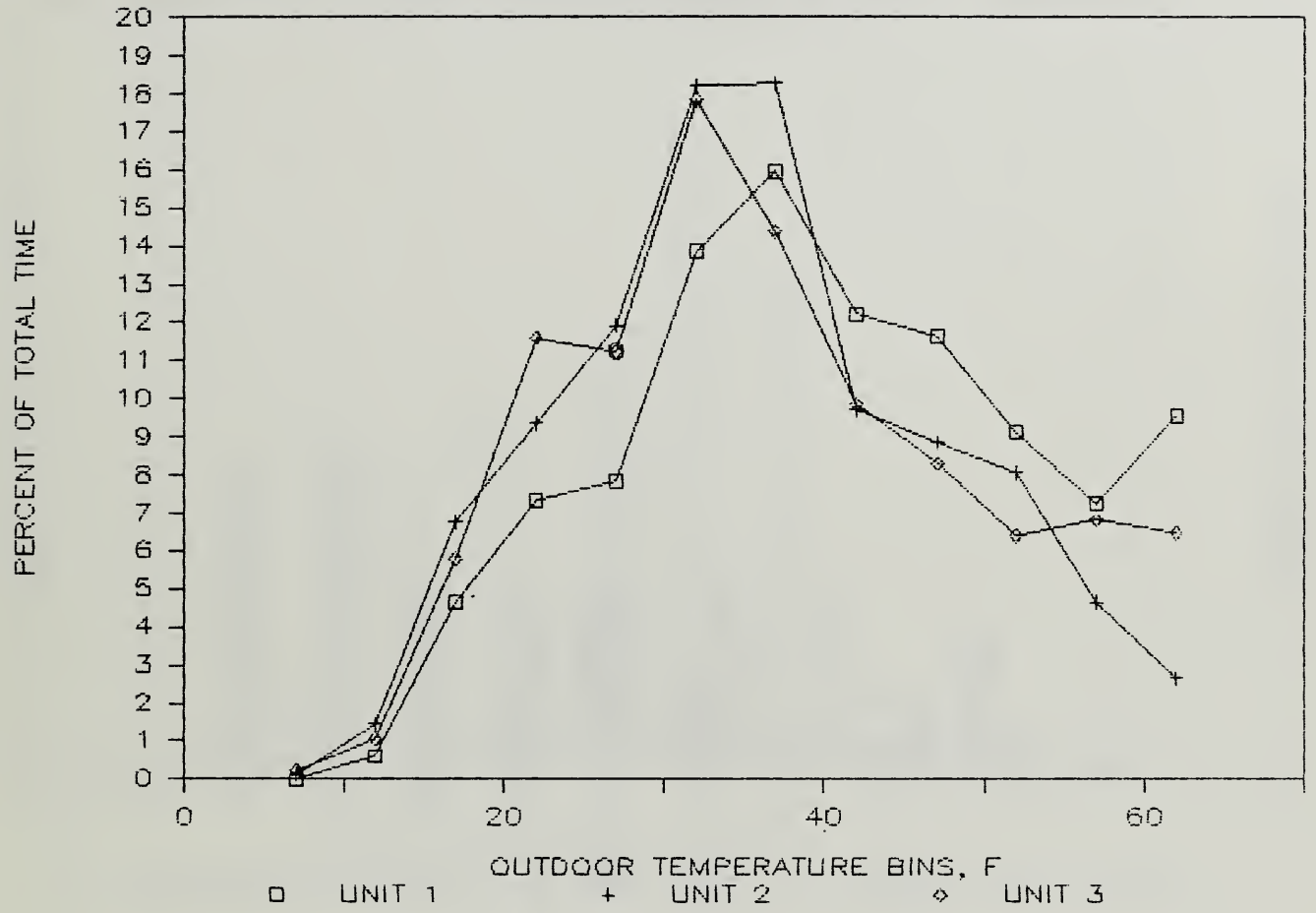

Figure 4.4 Outdoor Temperature Distribution

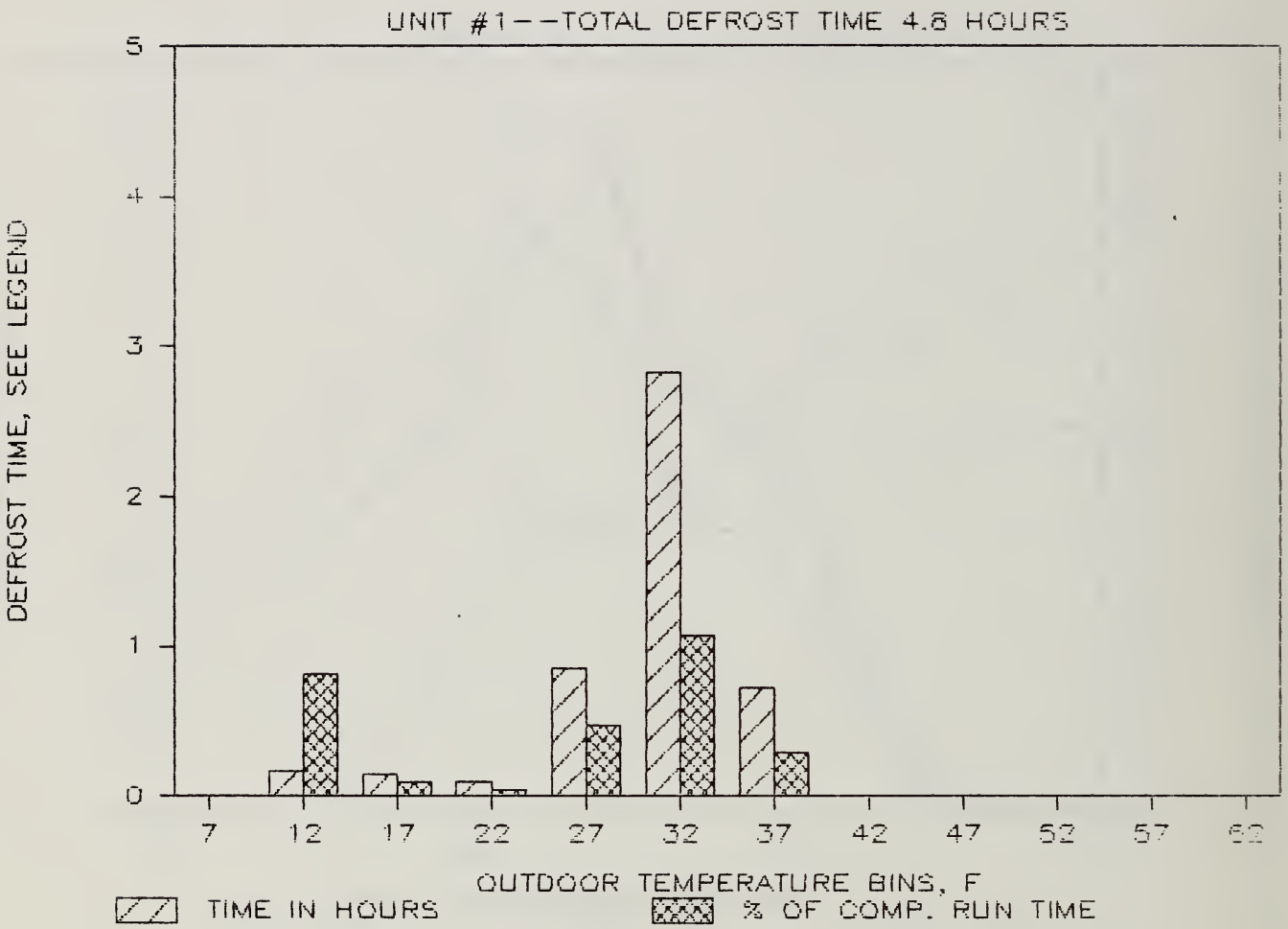

Figure 4.5 Defrost Time - Unit 1

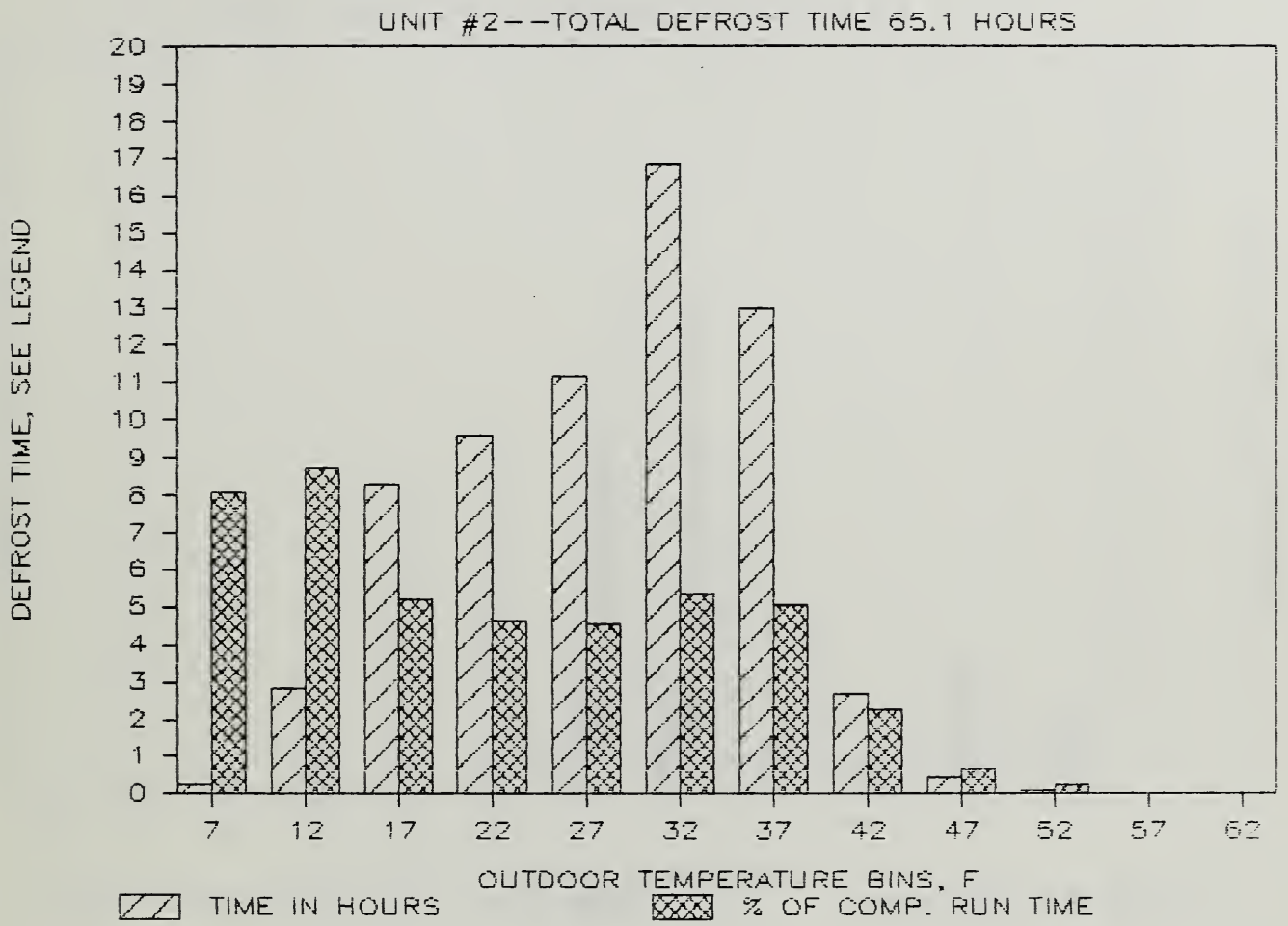

Figure 4.6 Defrost Time - Unit 2

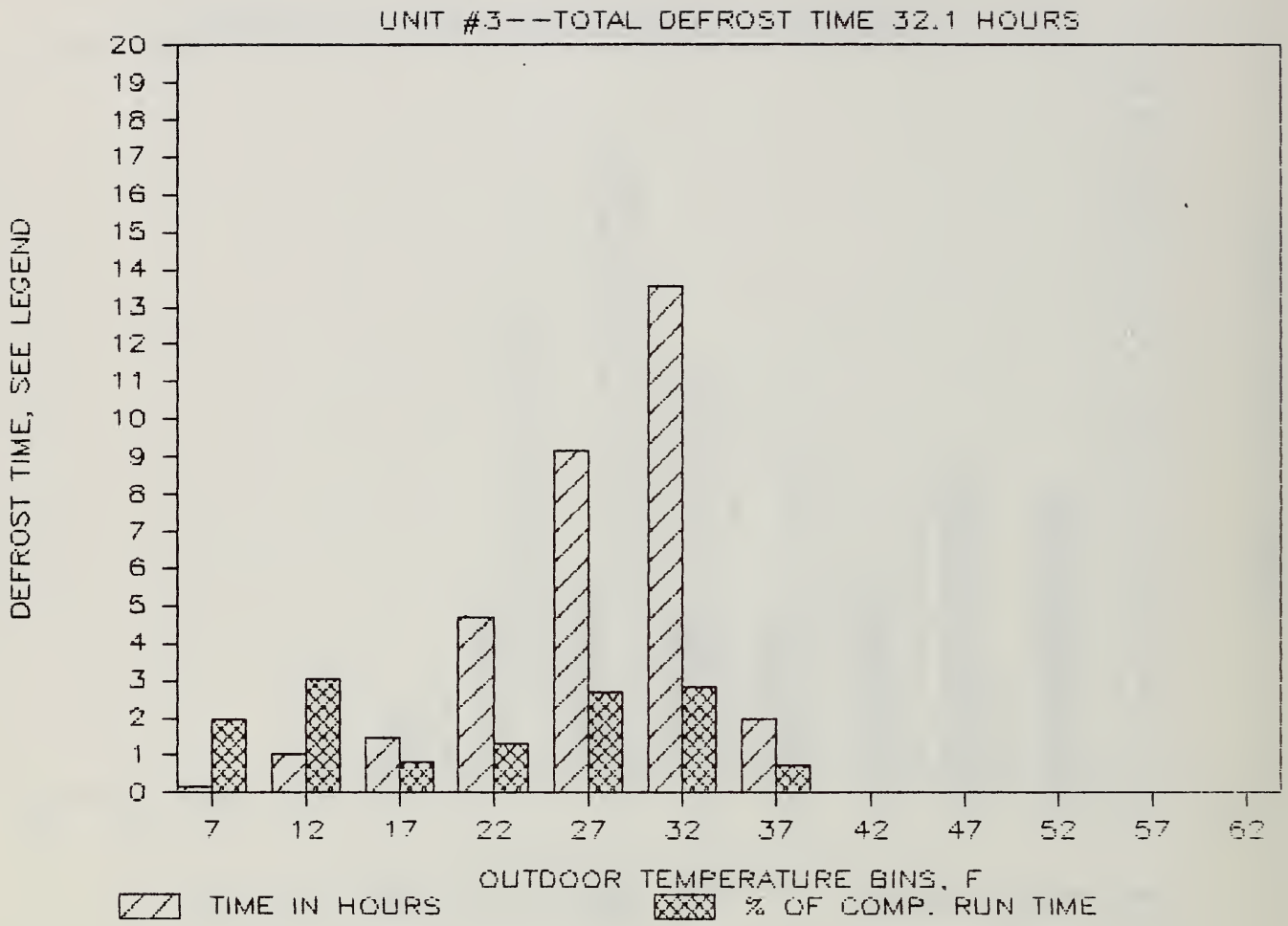

Figure 4.7 Defrost Time - Unit 3

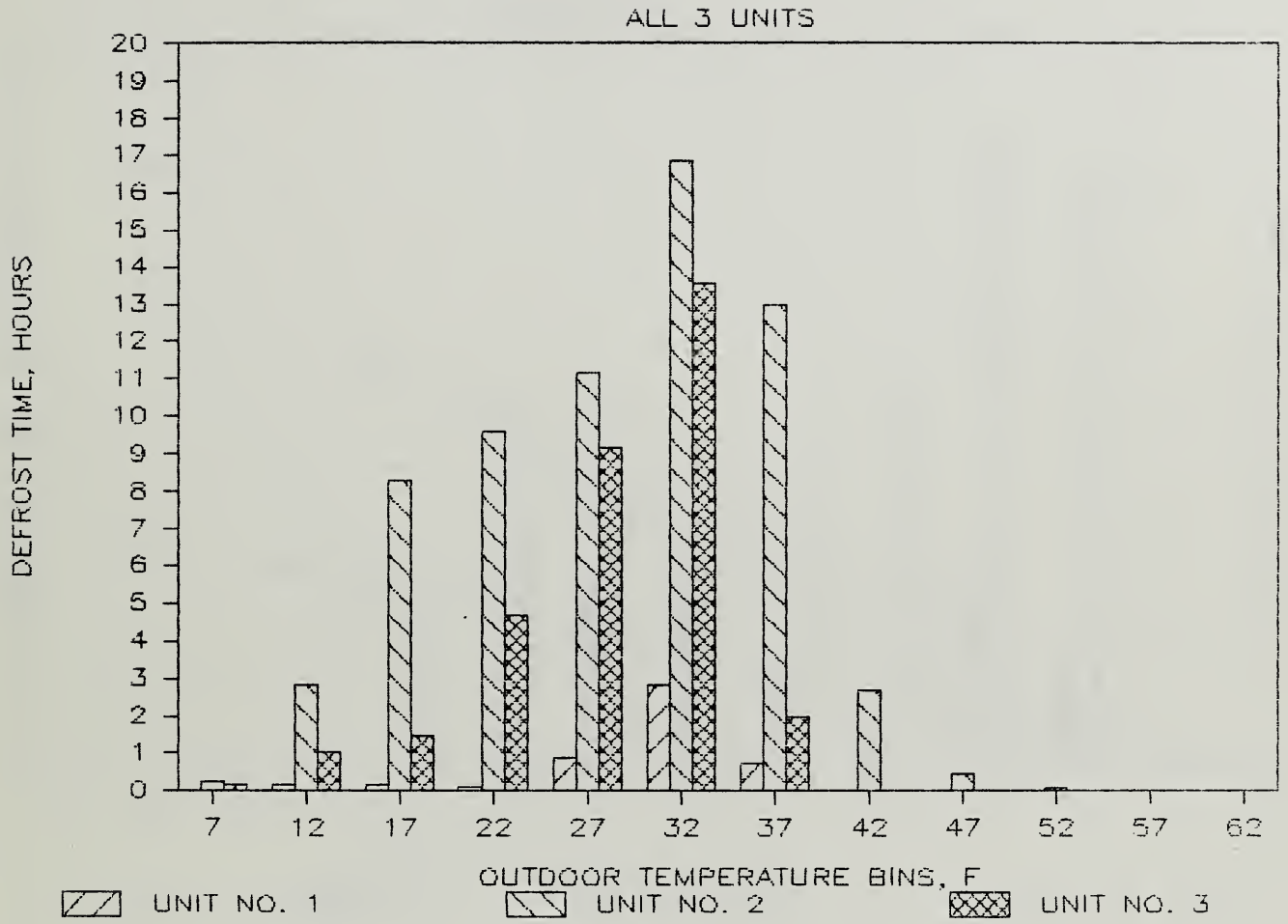

Figure 4.8 Defrost Time of Three Units (in hours)

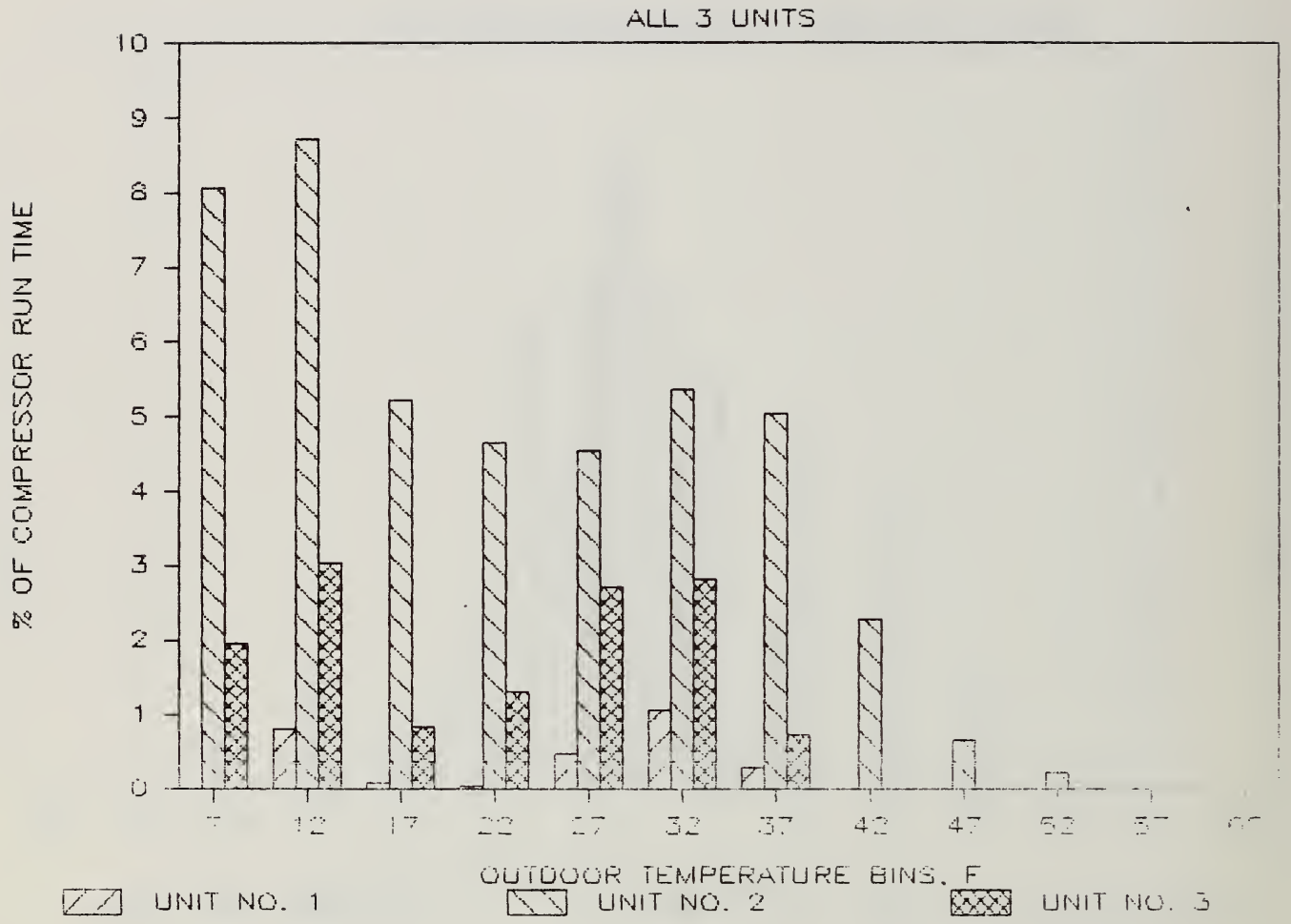

Figure 4.9 Defrost Time of Three Units (in % compressor run)

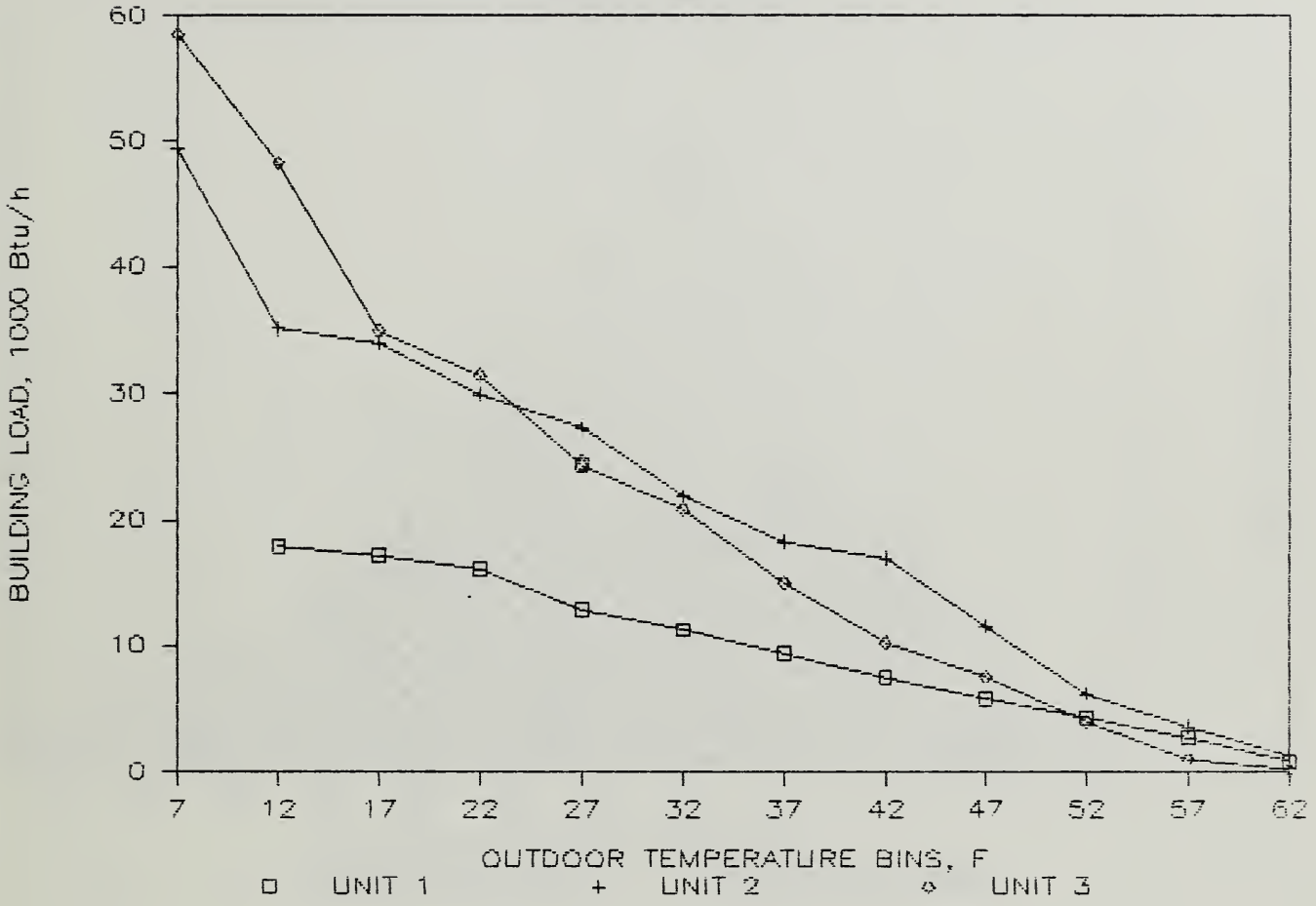

Figure 4.10 Building Loads

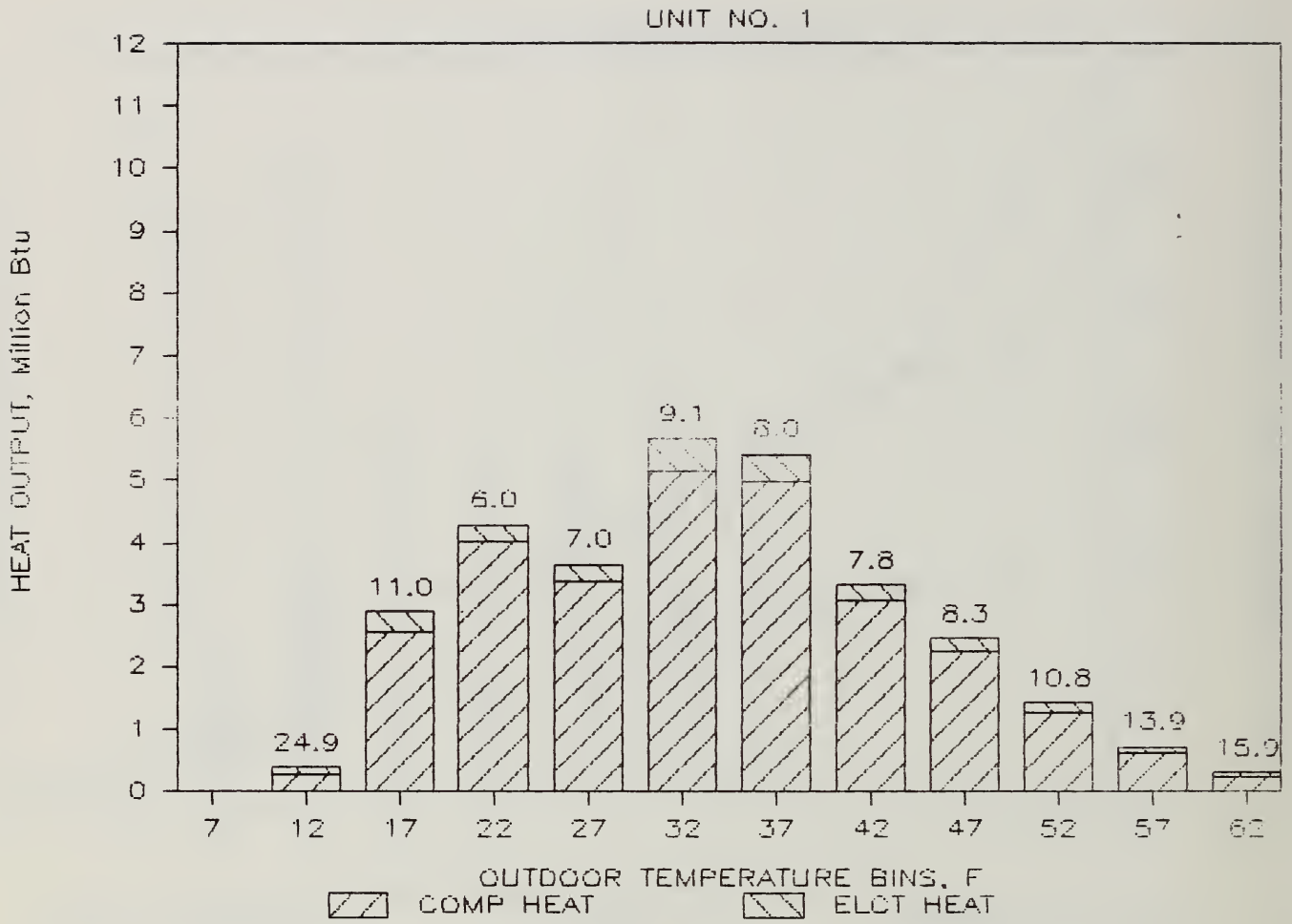

Figure 4.11 Heat Output vs. Outdoor Temperature - Unit 1

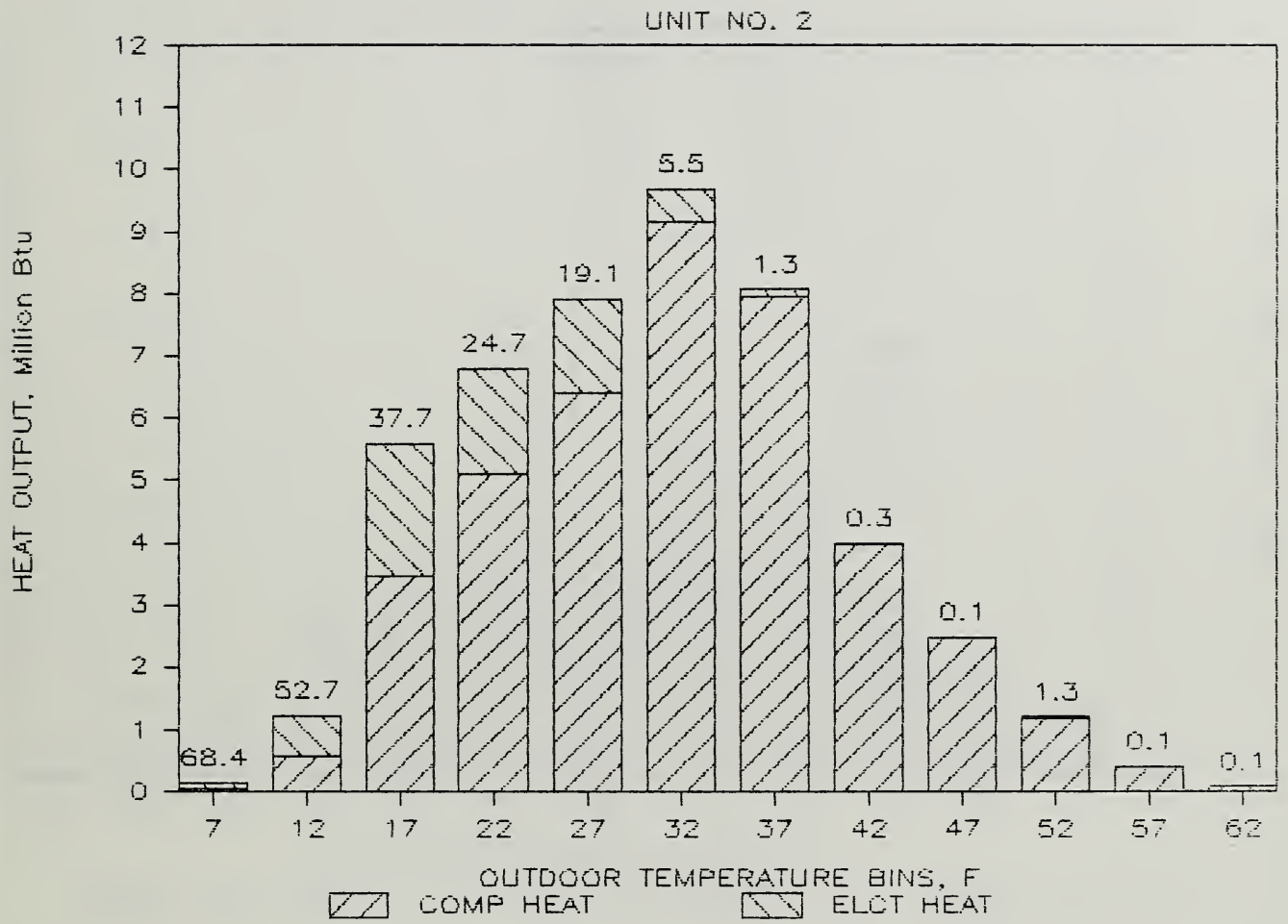

Figure 4.12 Heat Output vs. Outdoor Temperature - Unit 2

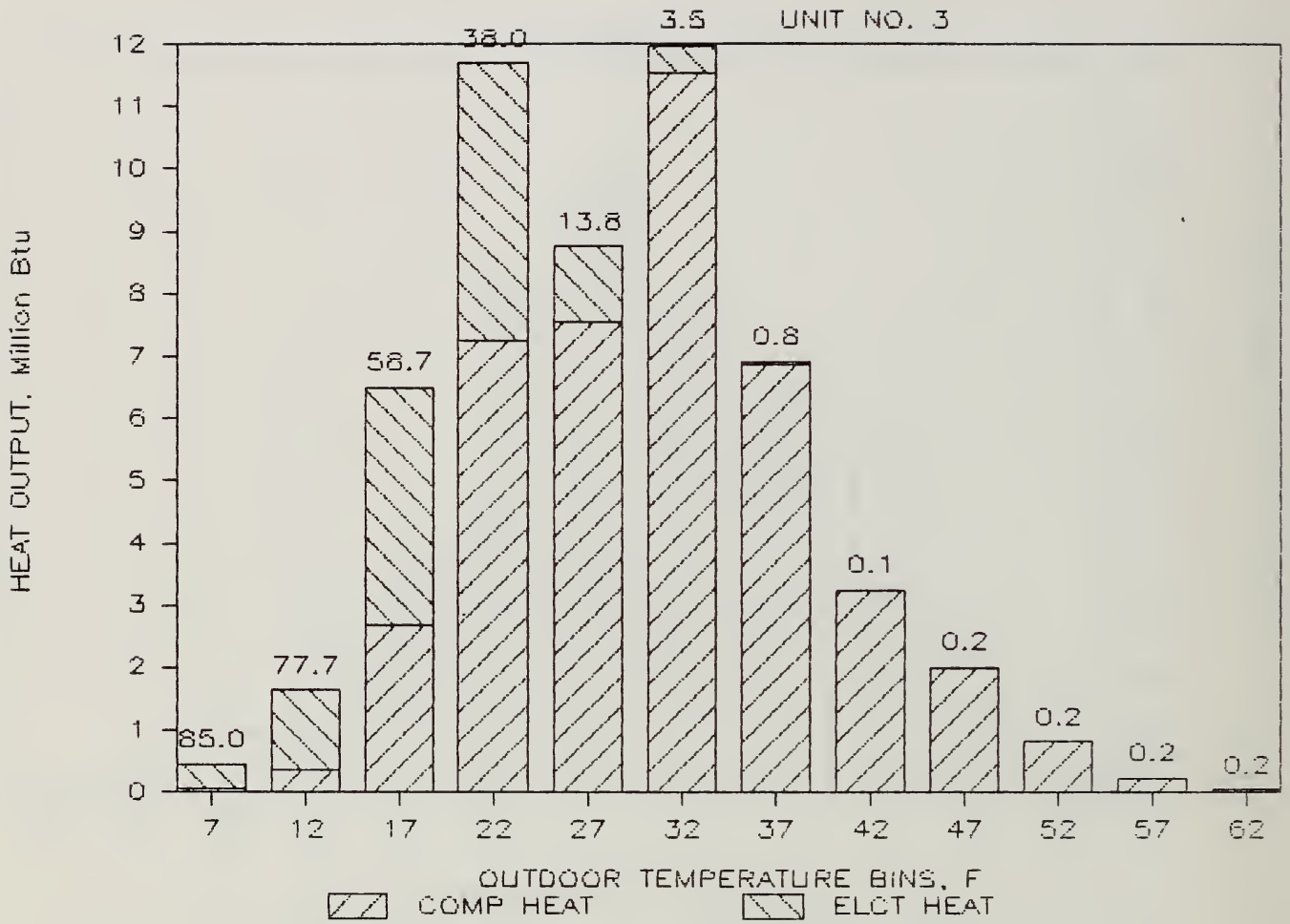

Figure 4.13 Heat Output vs. Outdoor Temperature - Unit 3

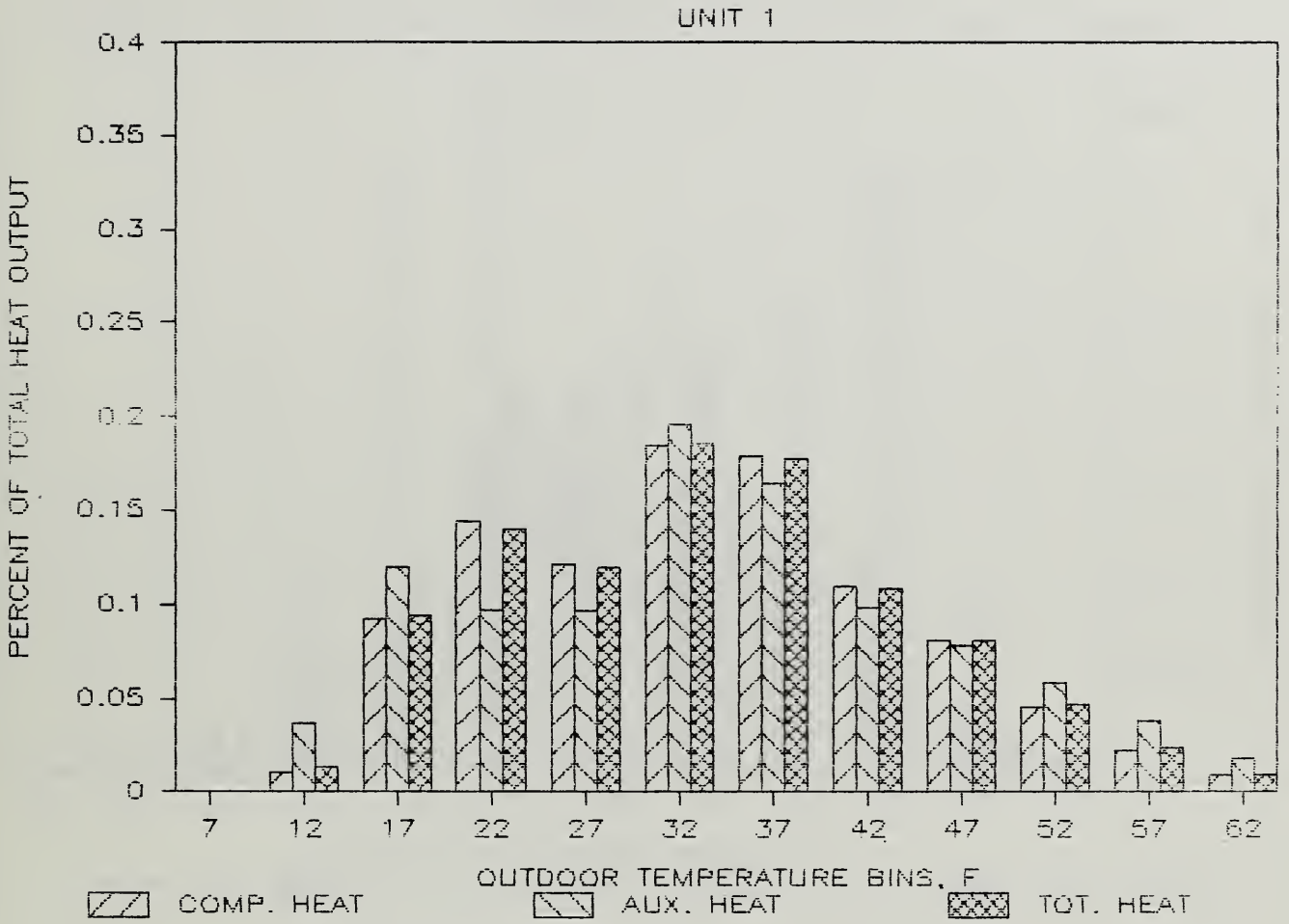

Figure 4.14 Percent Heat Output vs. Outdoor Temperature - Unit 1

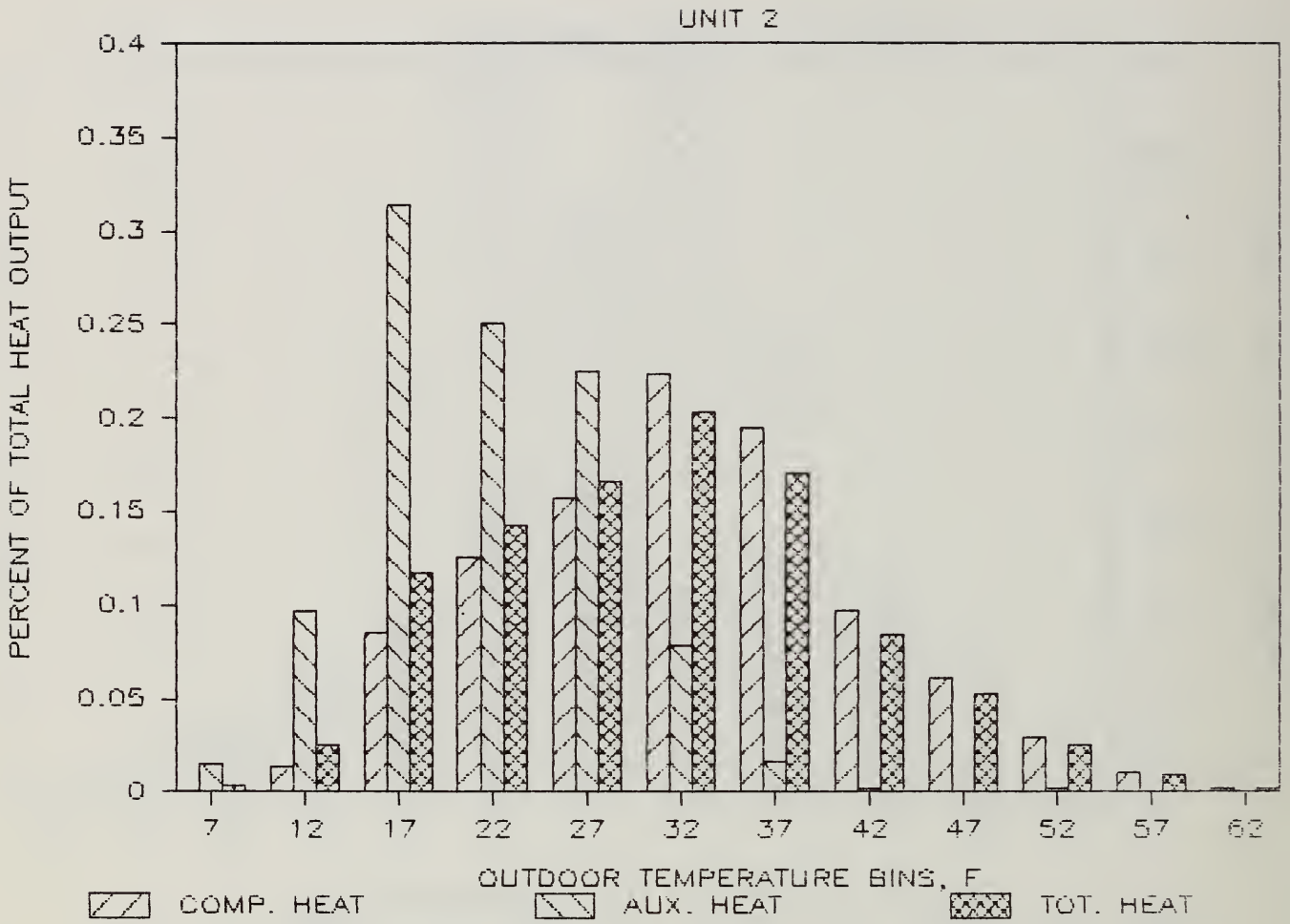

Figure 4.15 Percent Heat Output vs. Outdoor Temperature - Unit 2

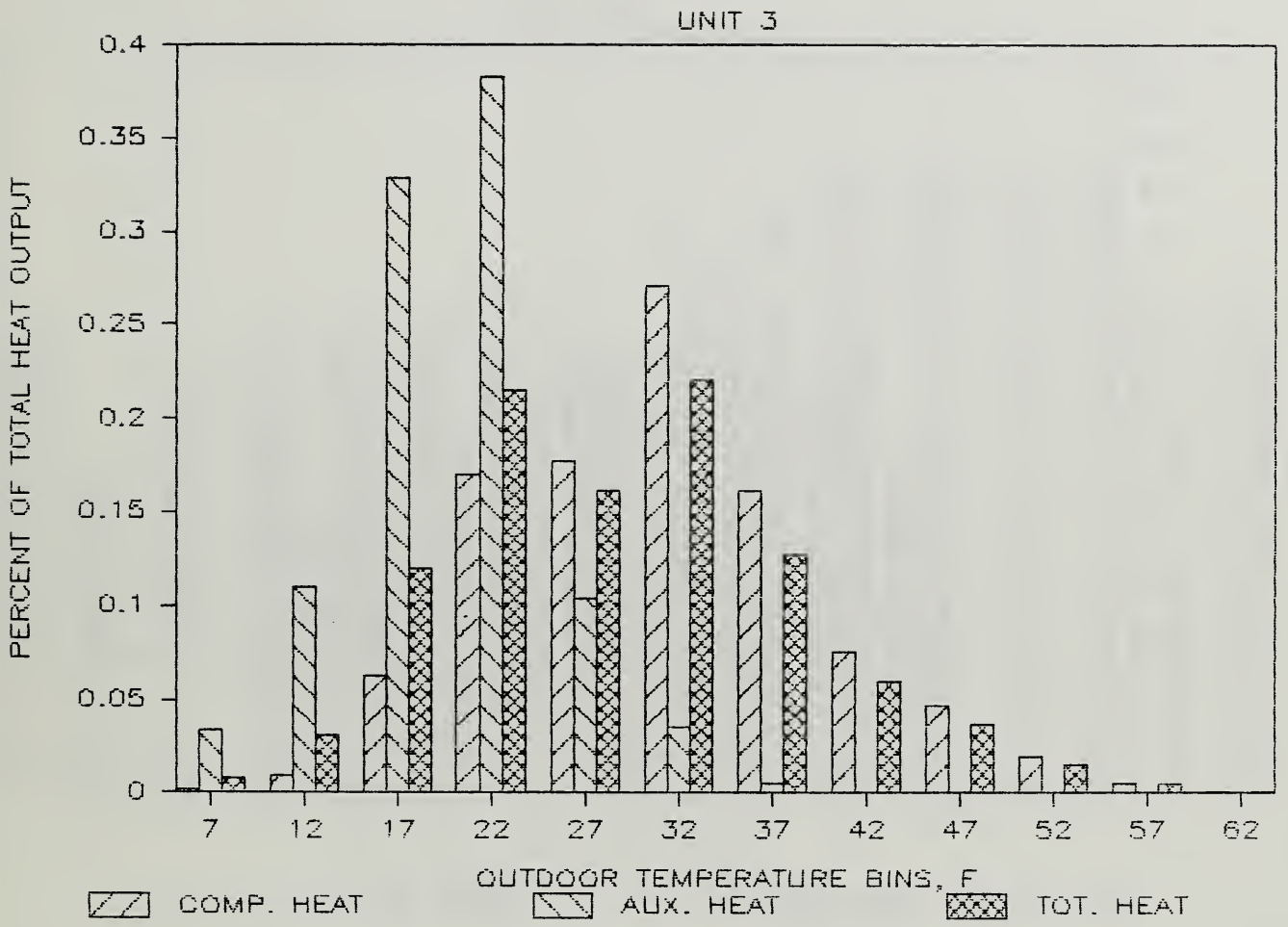

Figure 4.16 Percent Heat Output vs. Outdoor Temperature - Unit 3

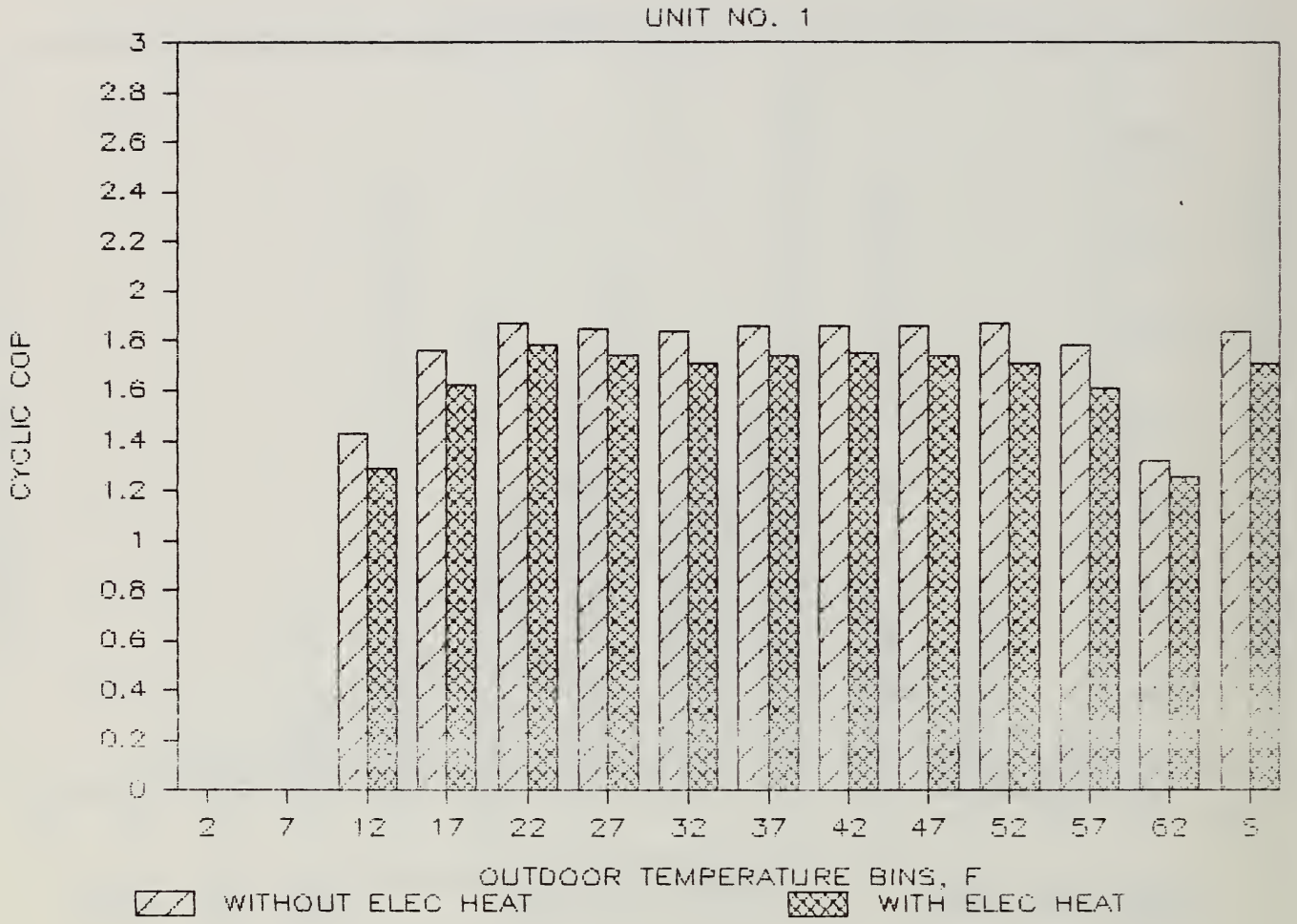

Figure 4.17 Cyclic COP vs. Outdoor Temperature - Unit 1

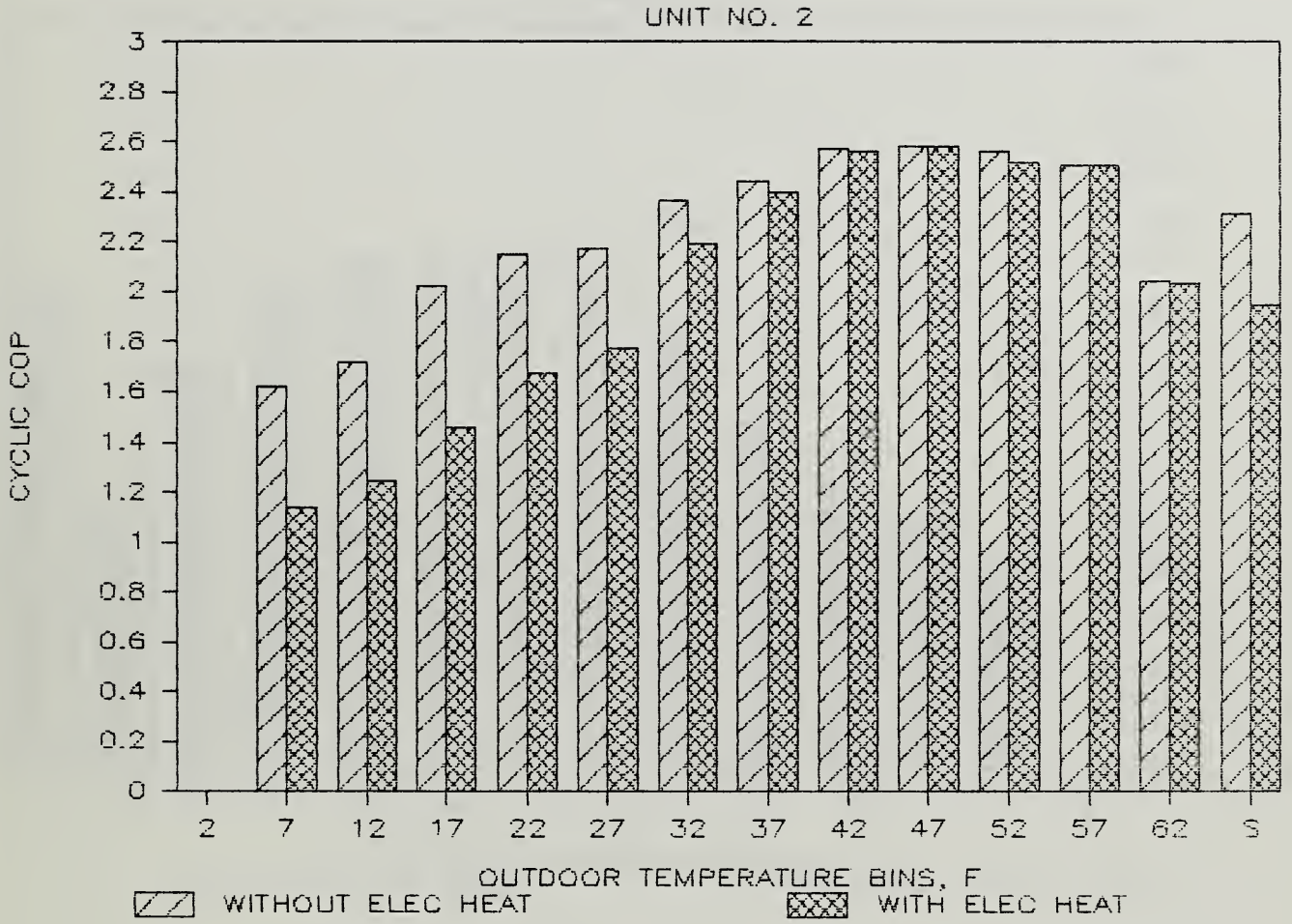

Figure 4.18 Cyclic COP vs. Outdoor Temperature - Unit 2

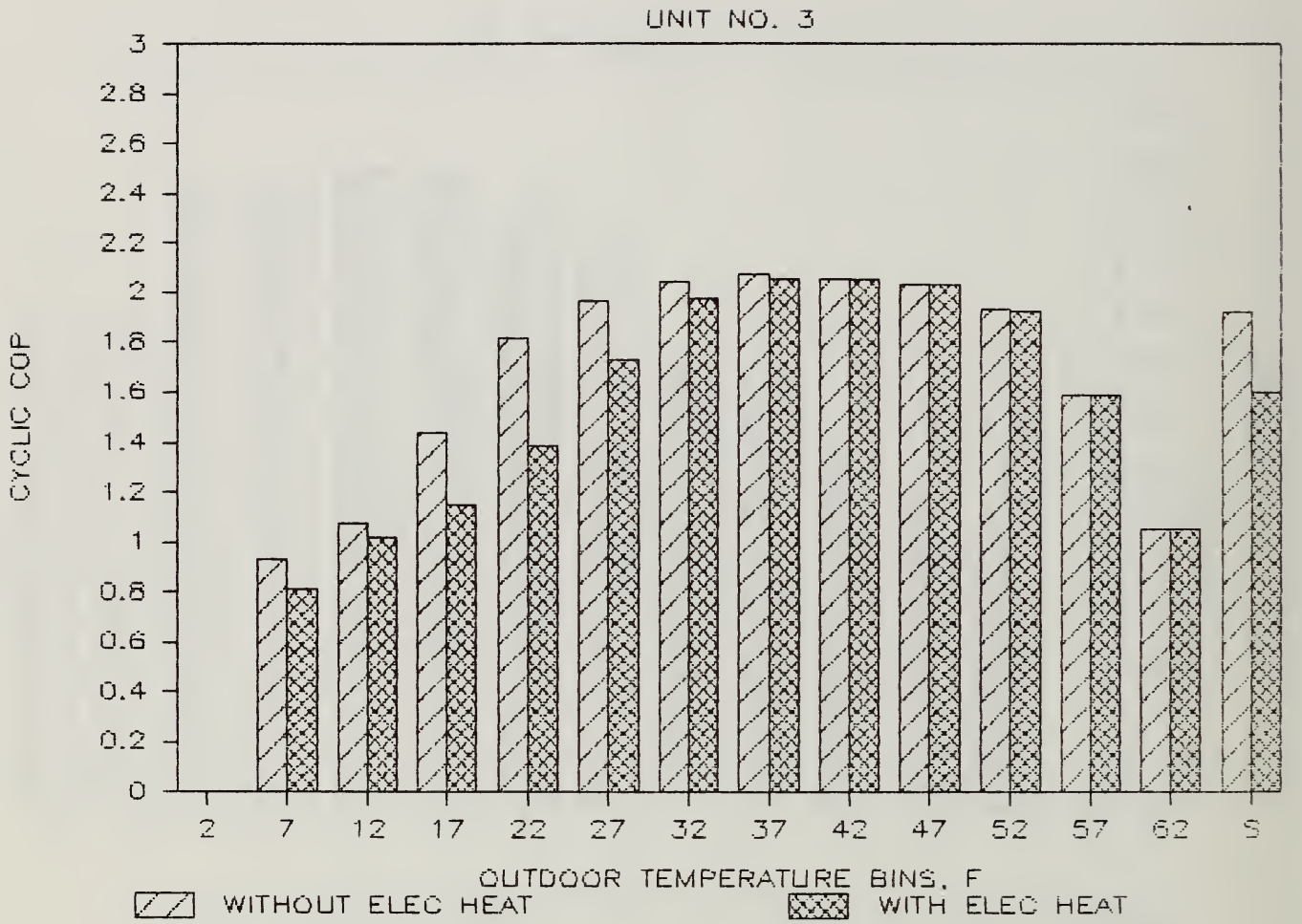

Figure 4.19 Cyclic COP vs. Outdoor Temperature - Unit 3

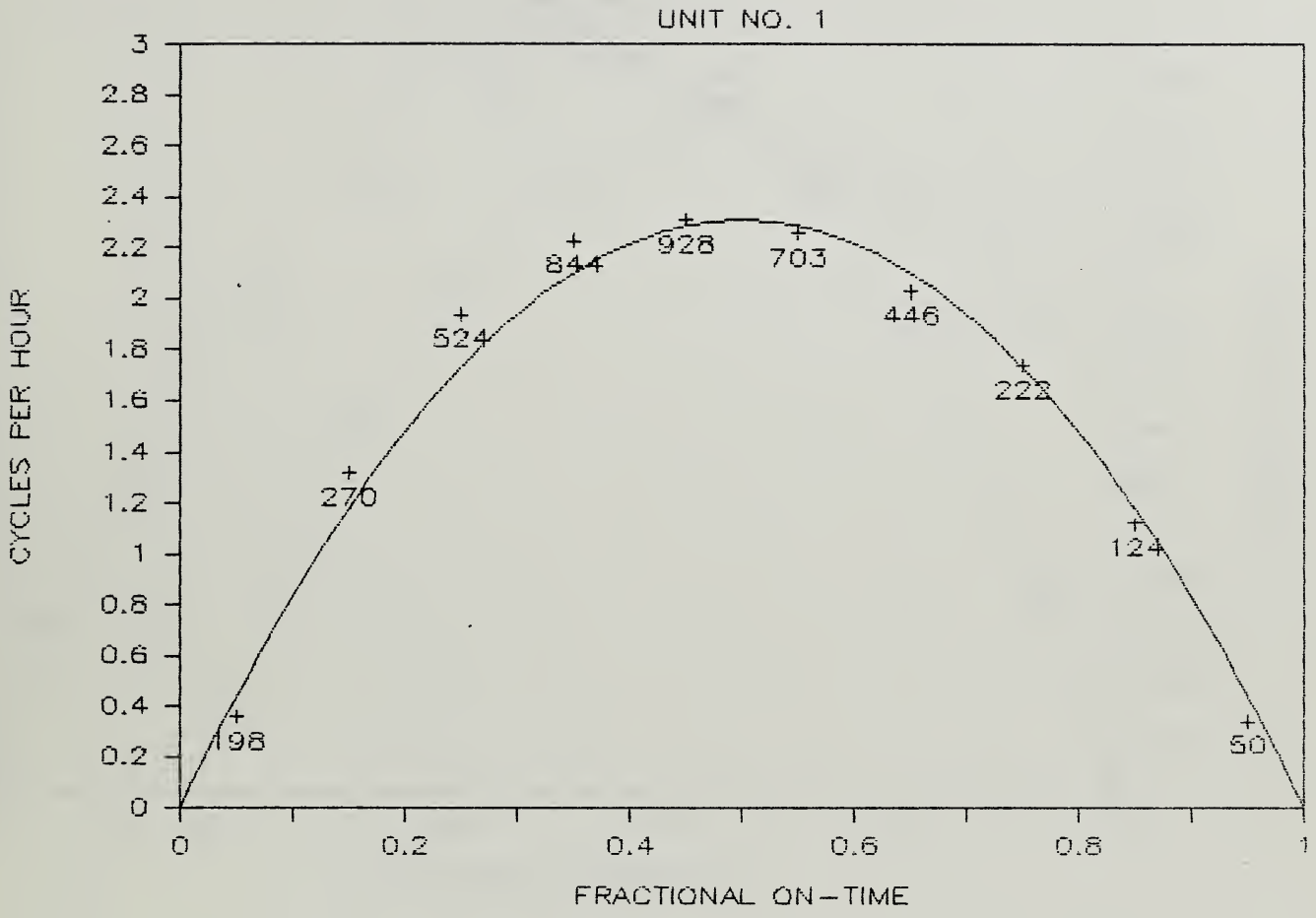

Figure 4.20 Compressor Cycling Rate - Unit 1

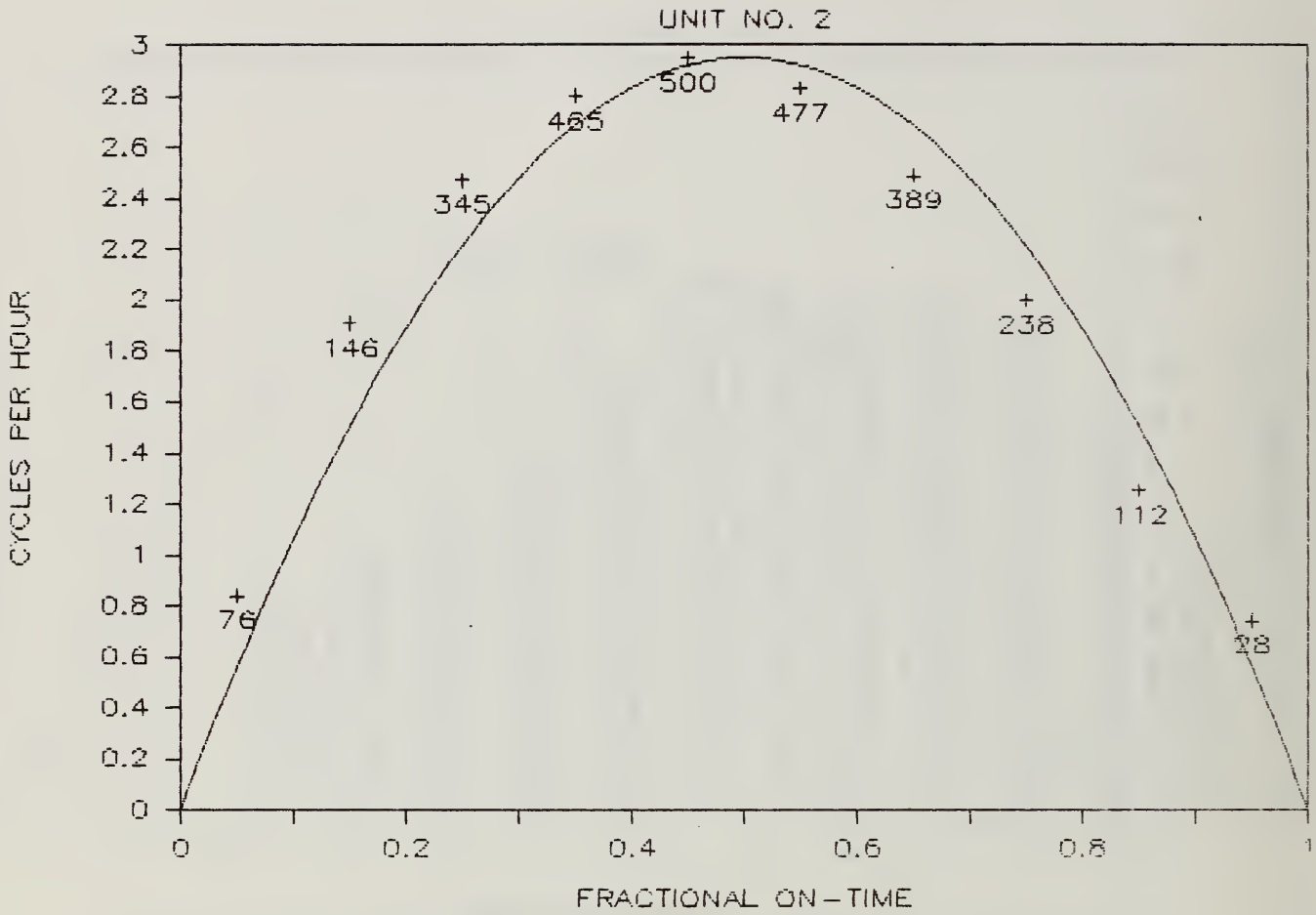

Figure 4.21 Compressor Cycling Rate - Unit 2

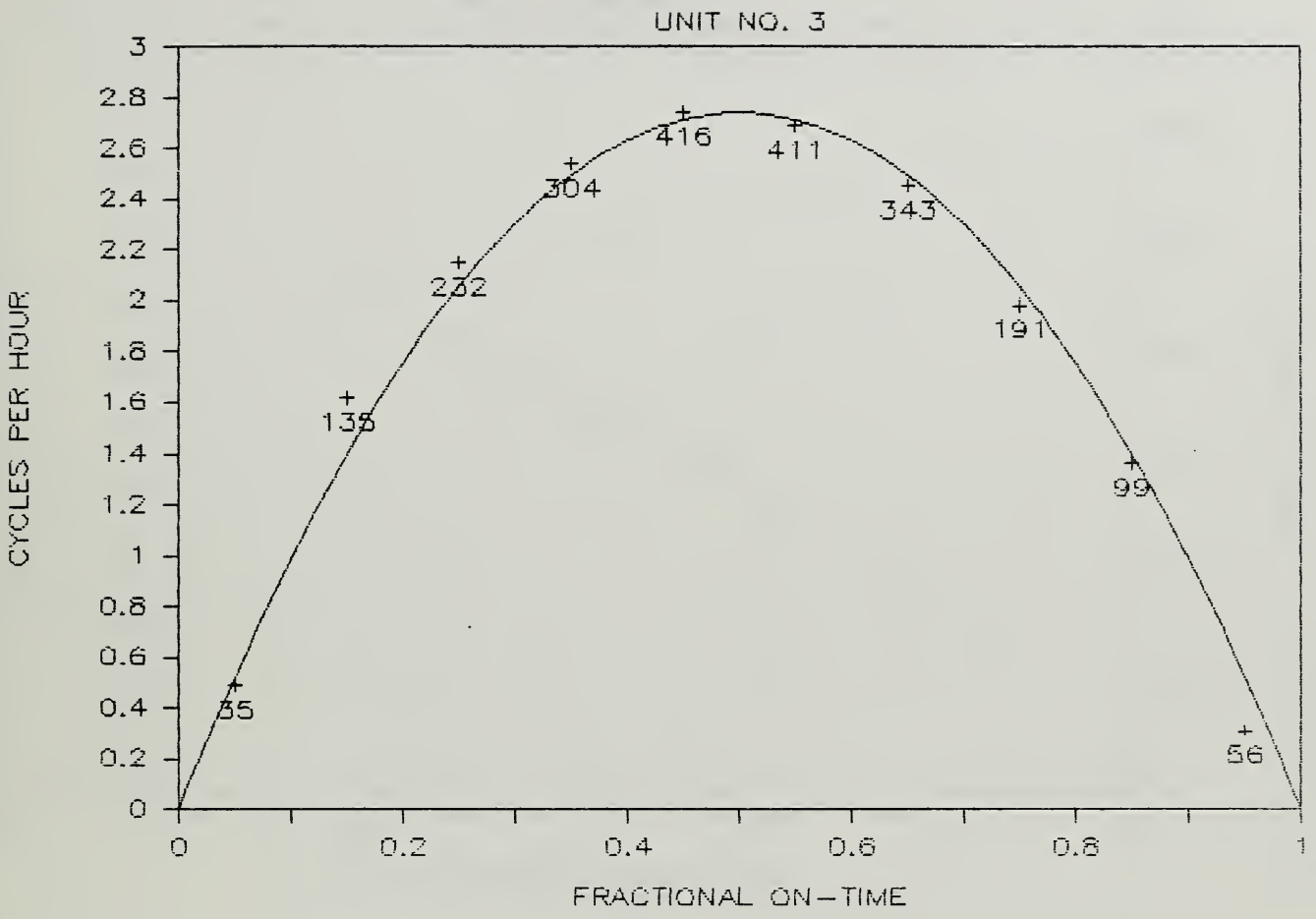

Figure 4.22 Compressor Cycling Rate - Unit 3

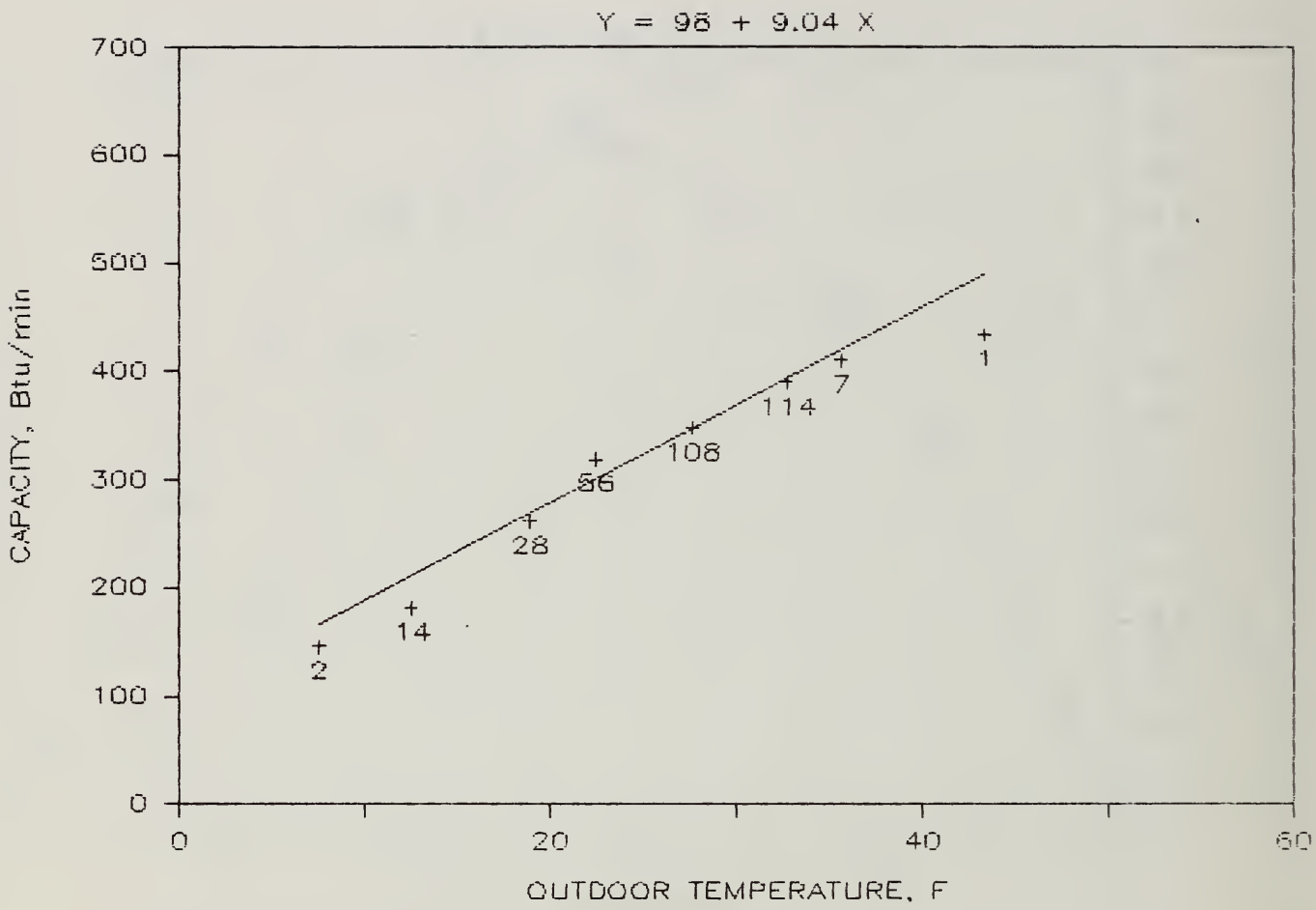

Figure 4.23 Capacity of Defrost Cycles - Unit 3

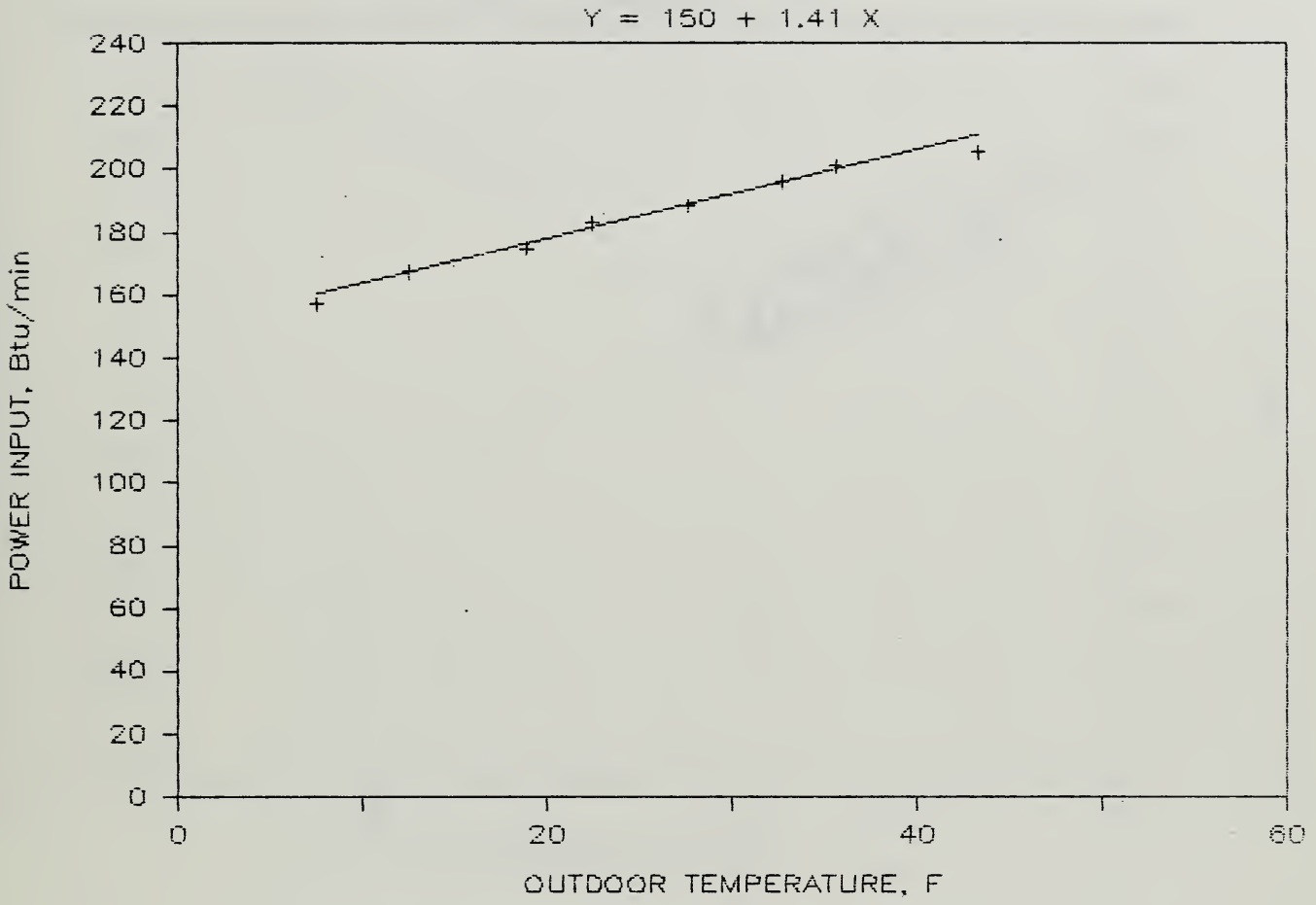

Figure 4.24 Power Input of Defrost Cycles - Unit 3

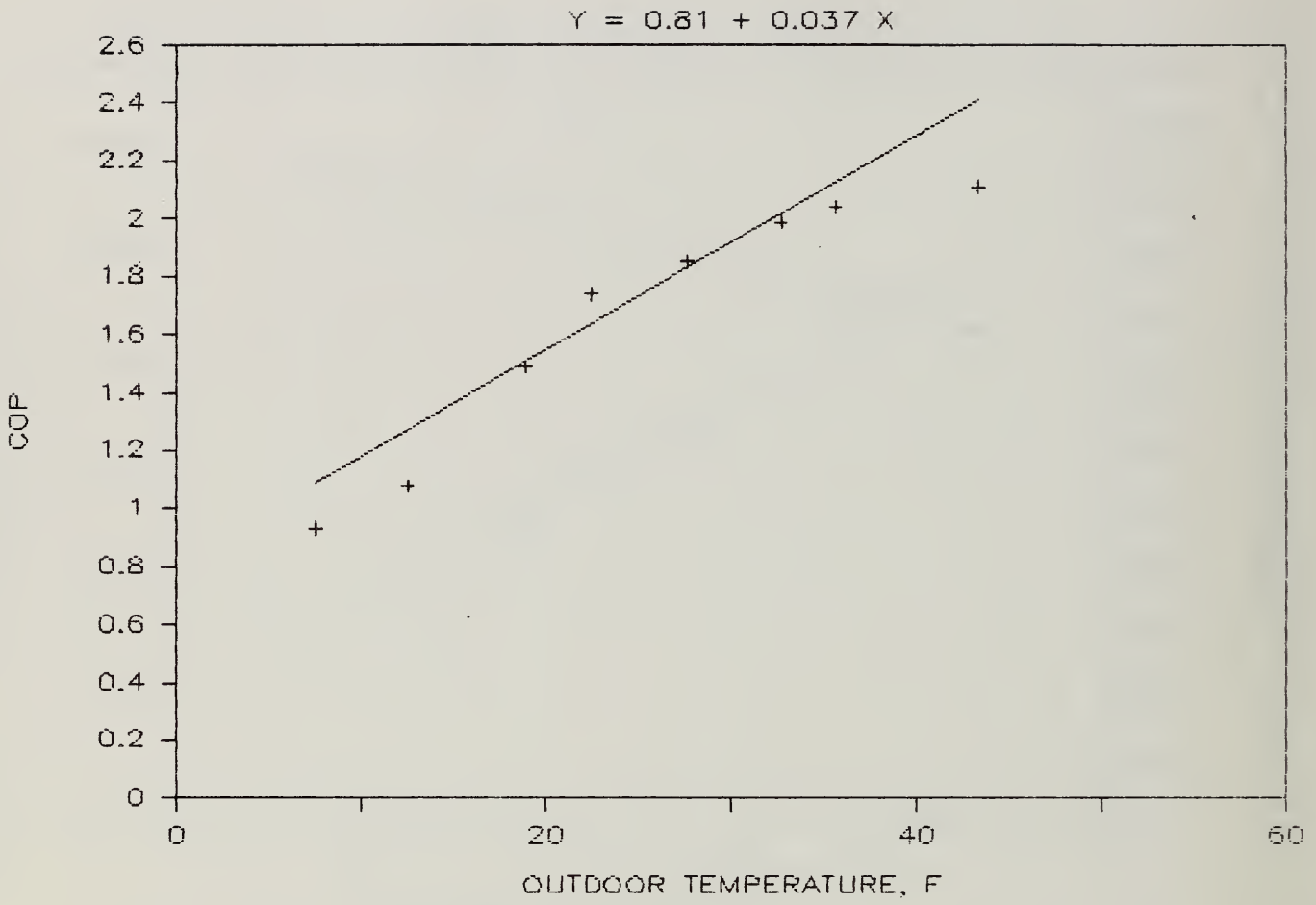

Figure 4.25 COP of Defrost Cycles - Unit 3

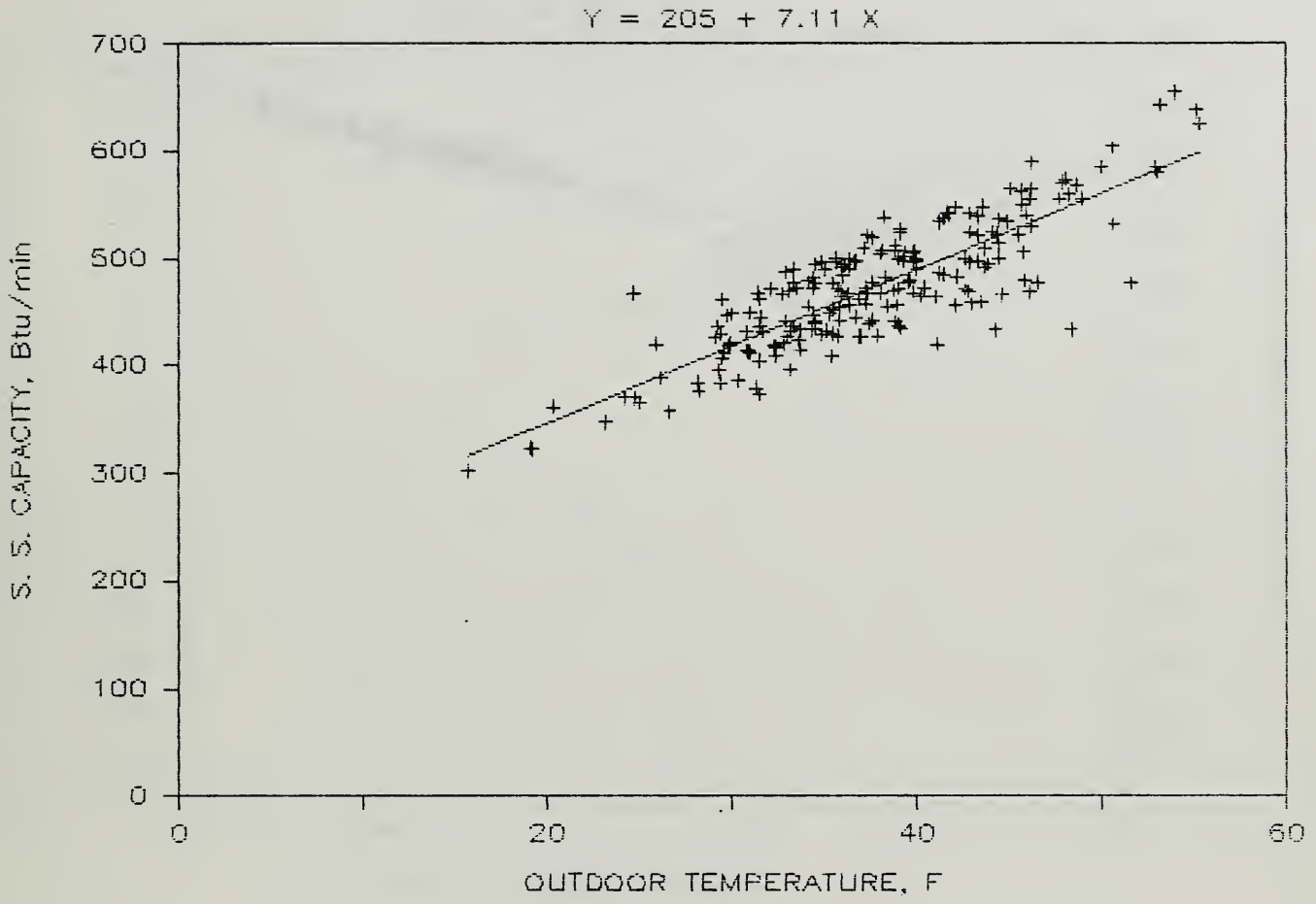

Figure 4.26 Steady State Capacity - Unit 3

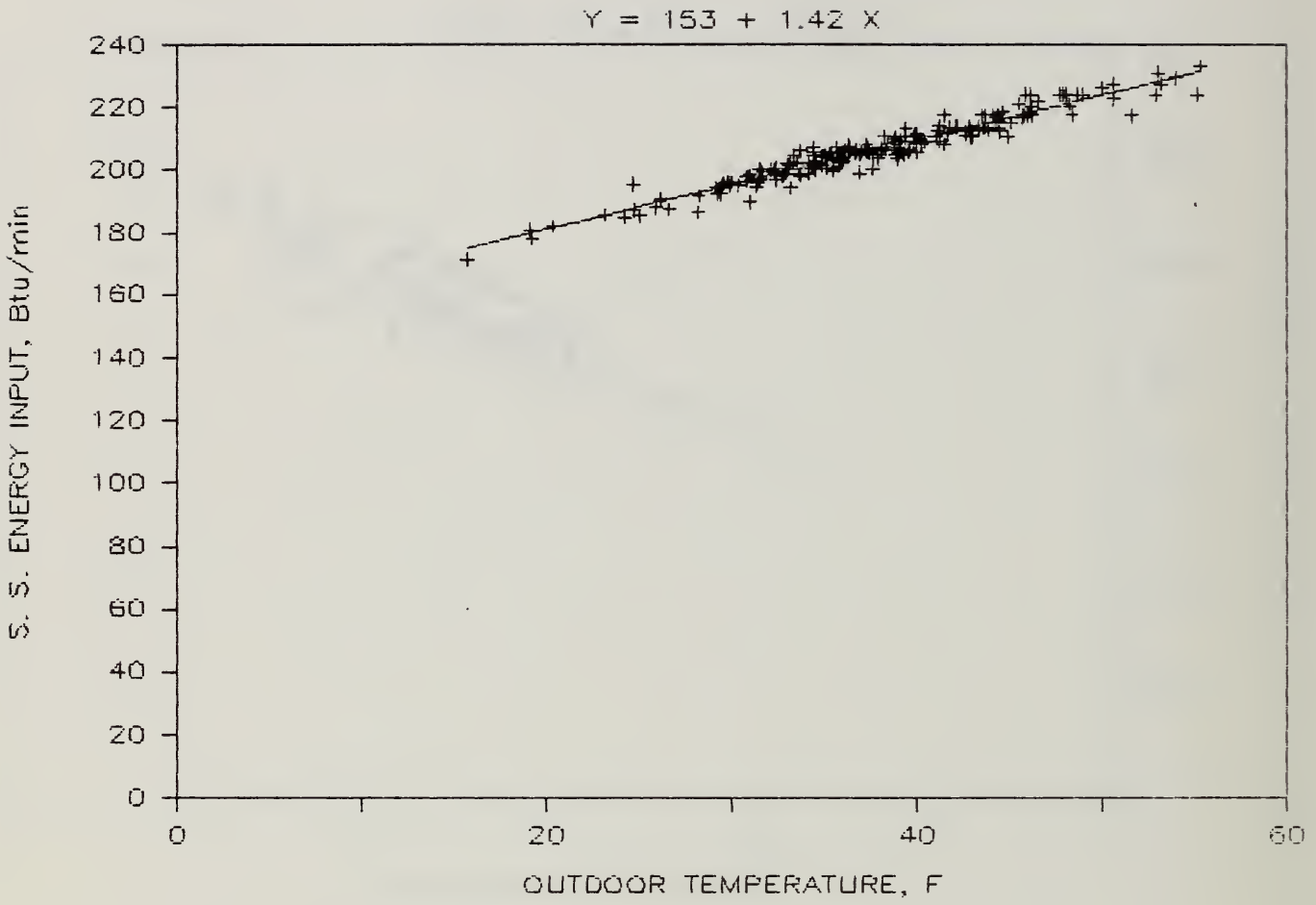

Figure 4.27 Steady State Power Input - Unit 3

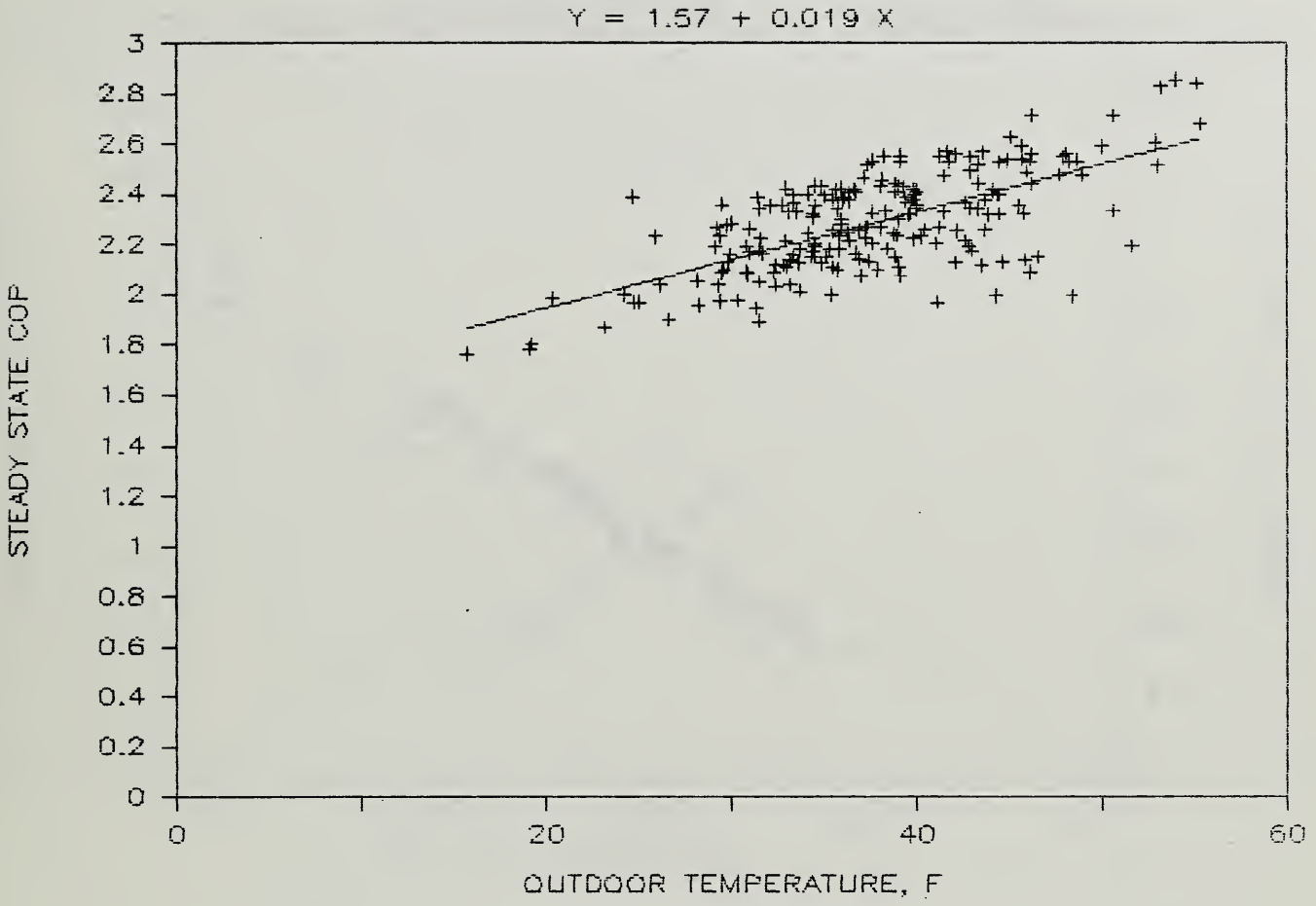

Figure 4.28 Steady State COP - Unit 3

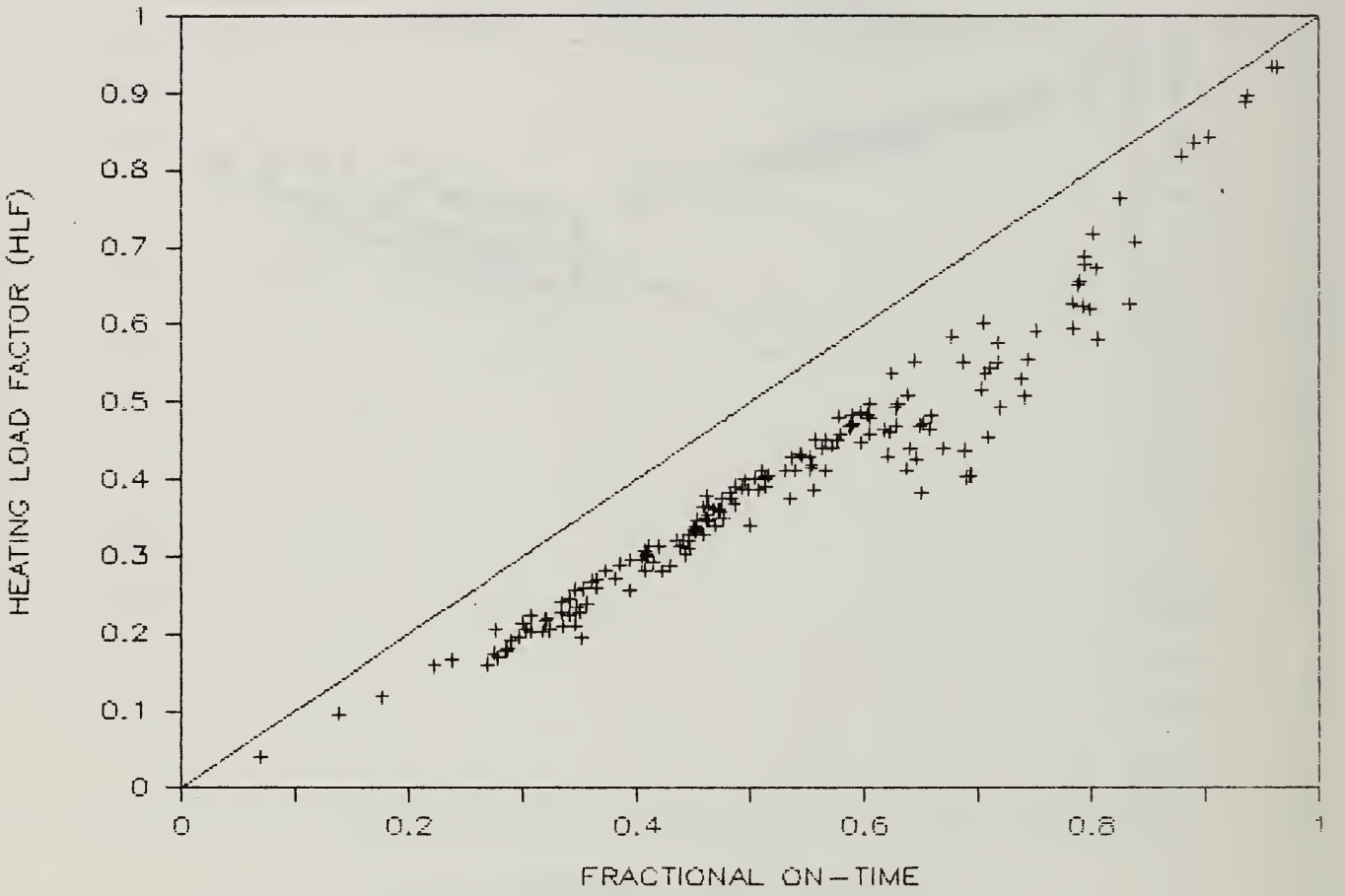

Figure 4.29 Heating Load Factor vs. Fractional On-Time - Unit 3 (all data available)

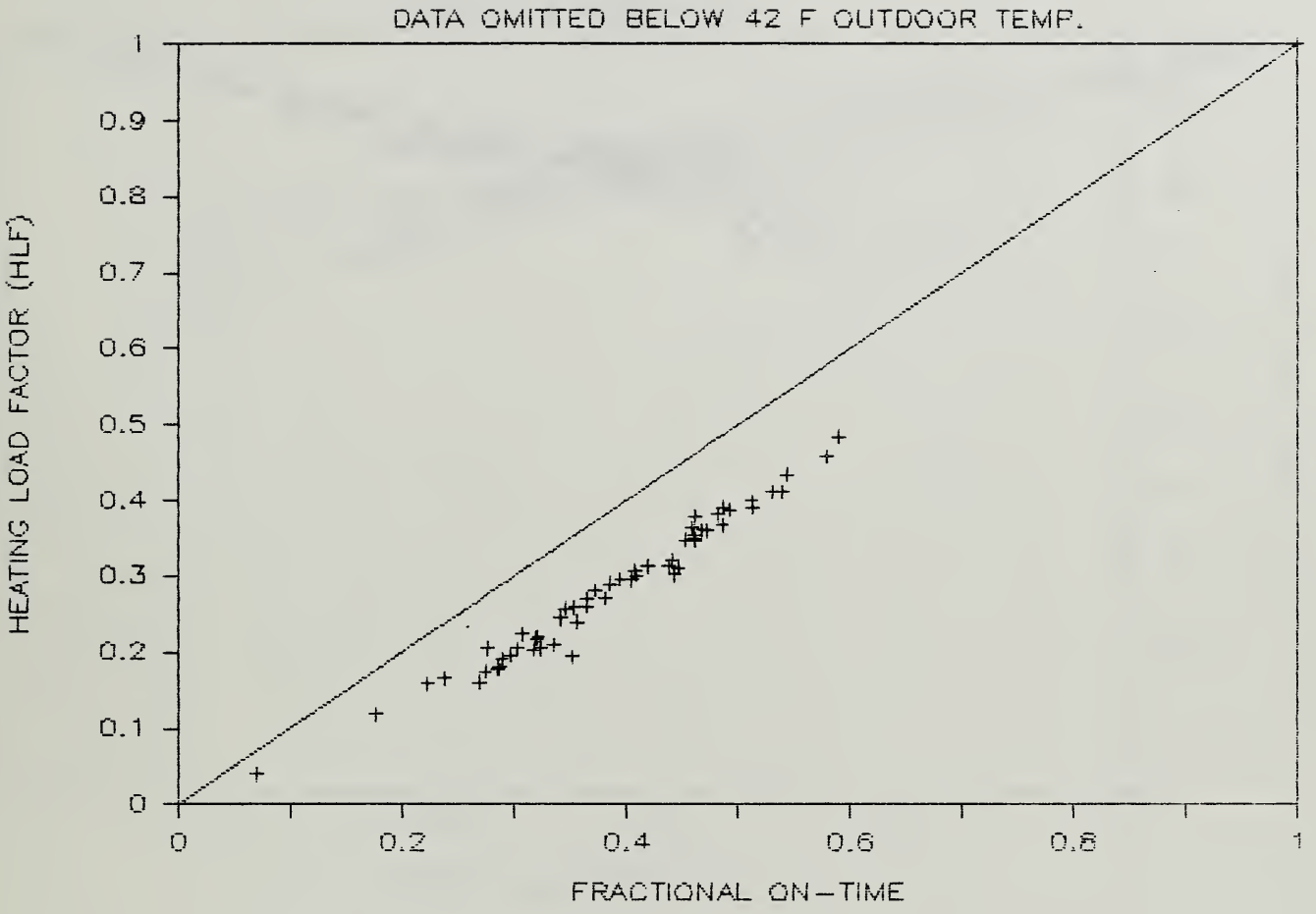

Figure 4.30 Heating Load Factor vs. Fractional On-Time - Unit 3 (data omitted below 42°F outdoor temperature)

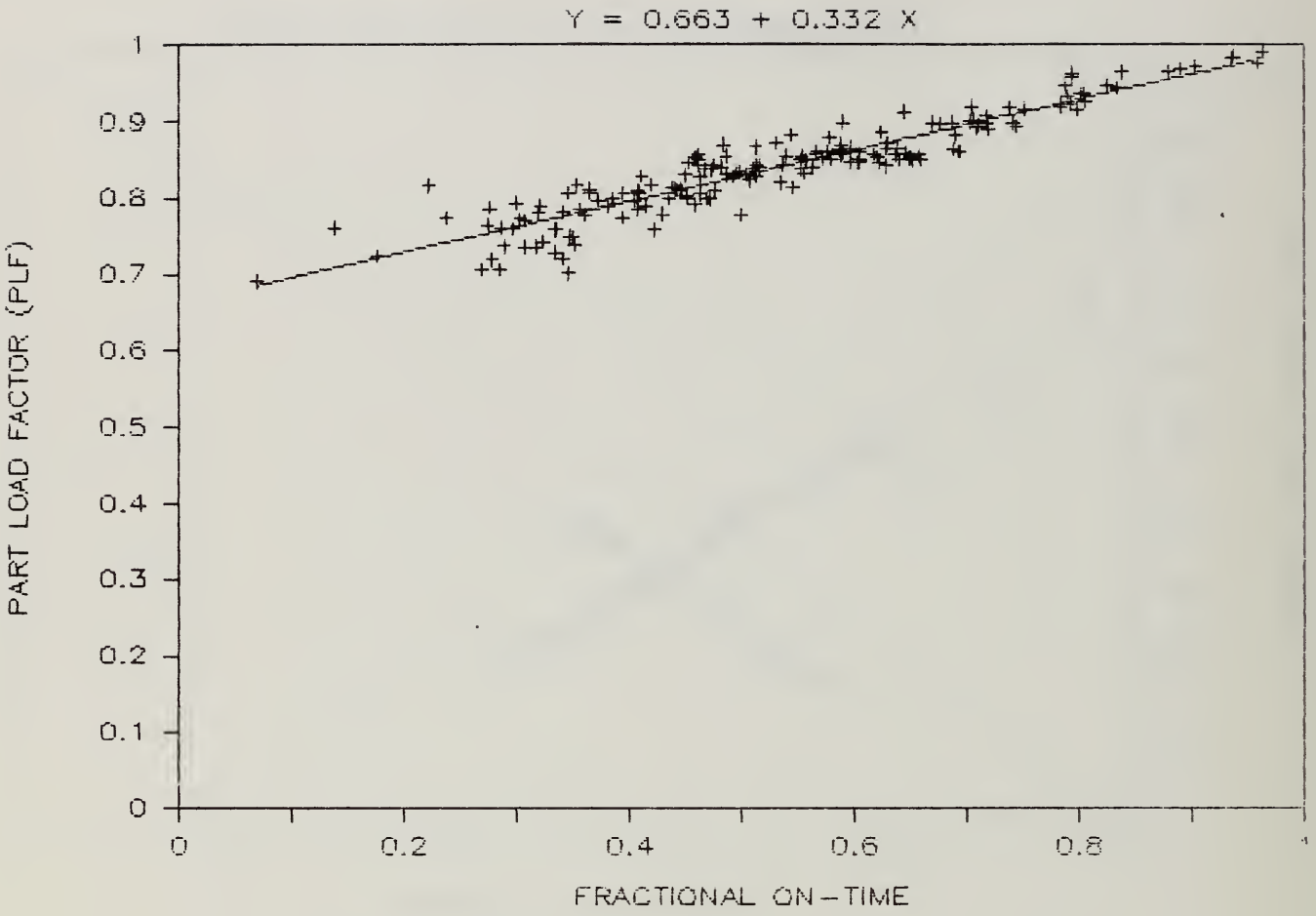

Figure 4.31 Part Load Factor vs. Fractional On-Time - Unit 3

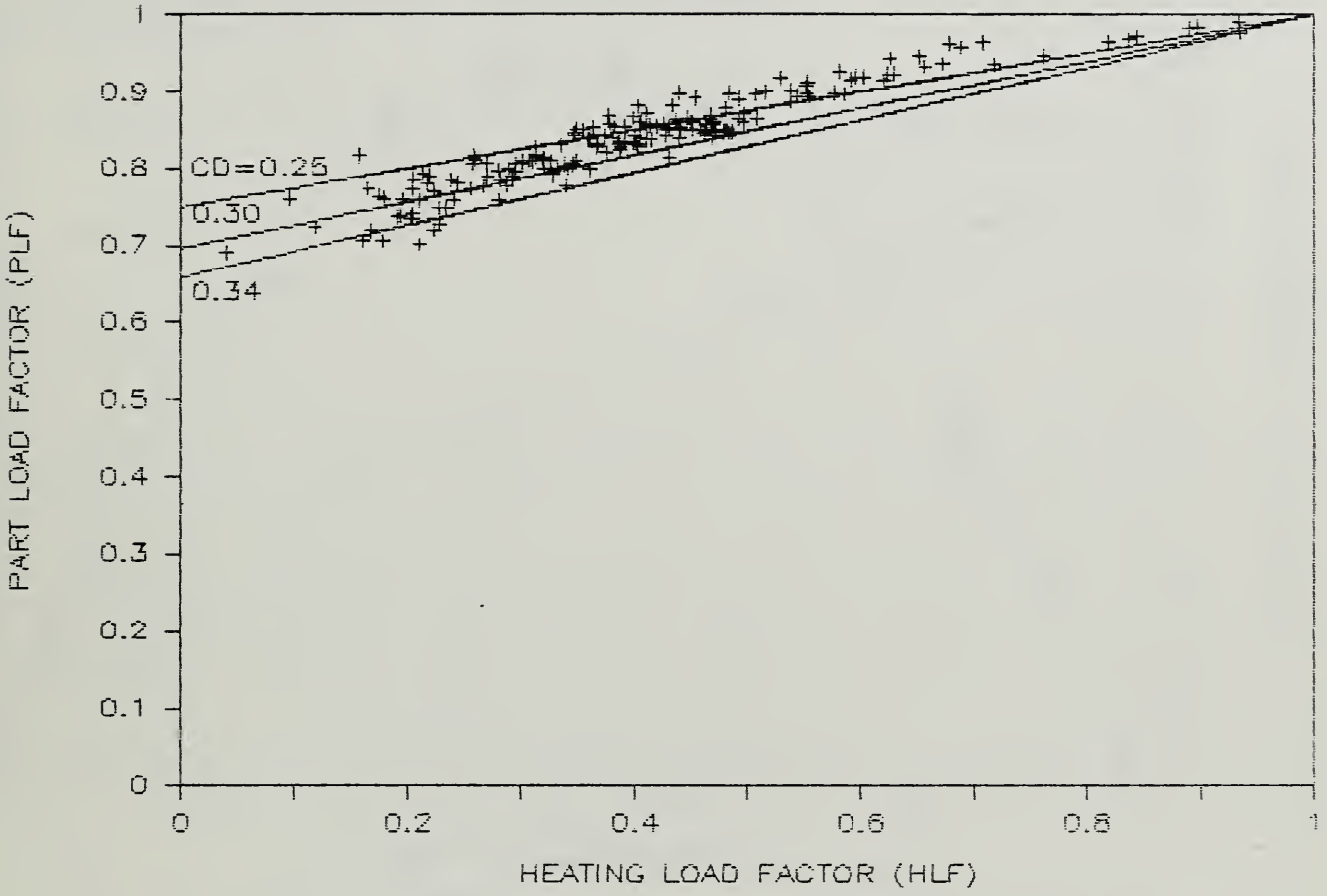

Figure 4.32 Part Load Factor vs. Heating Load Factor - Unit 3

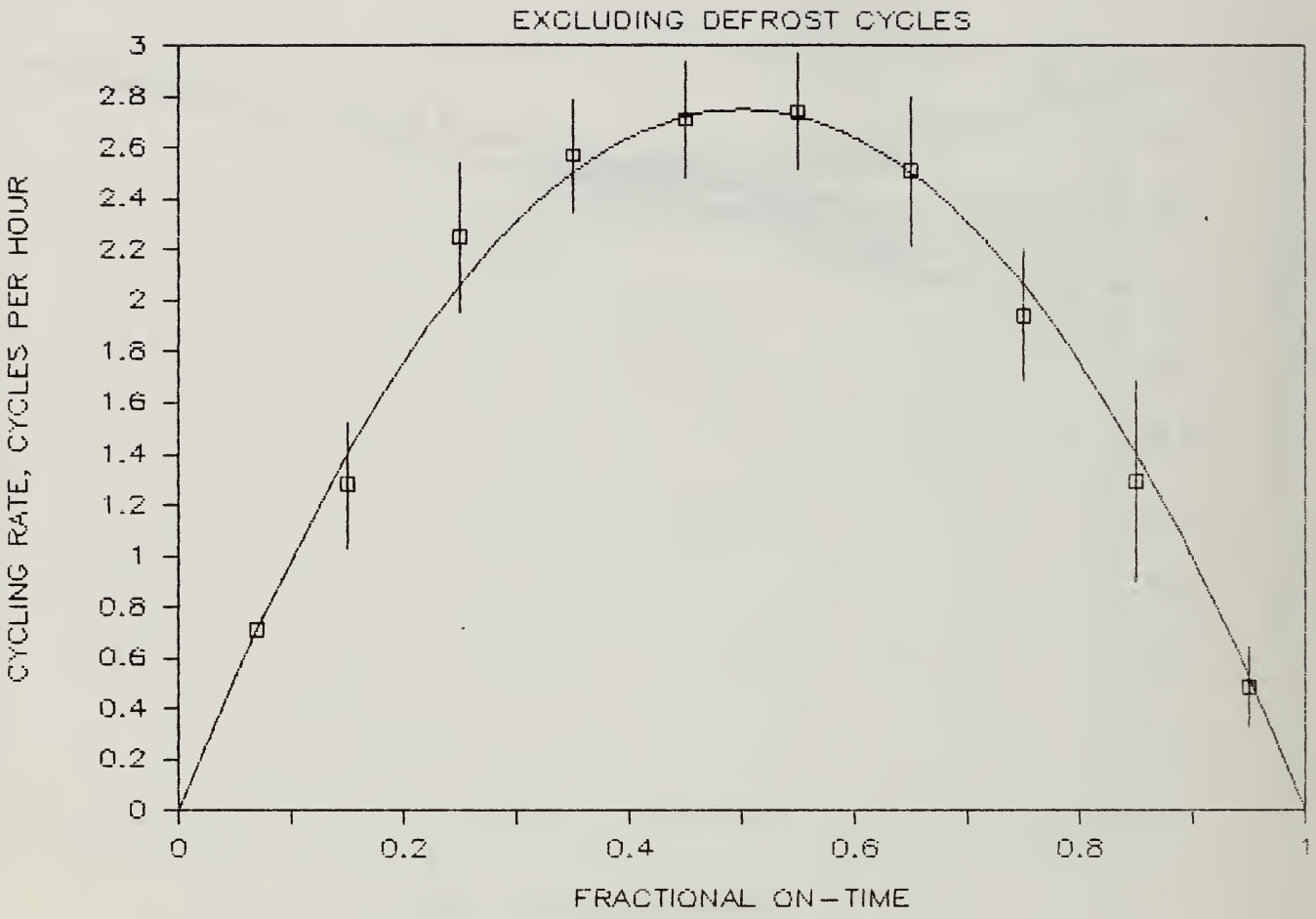

Figure 4.33 Cycling Rate (excluding defrost cycles) - Unit 3

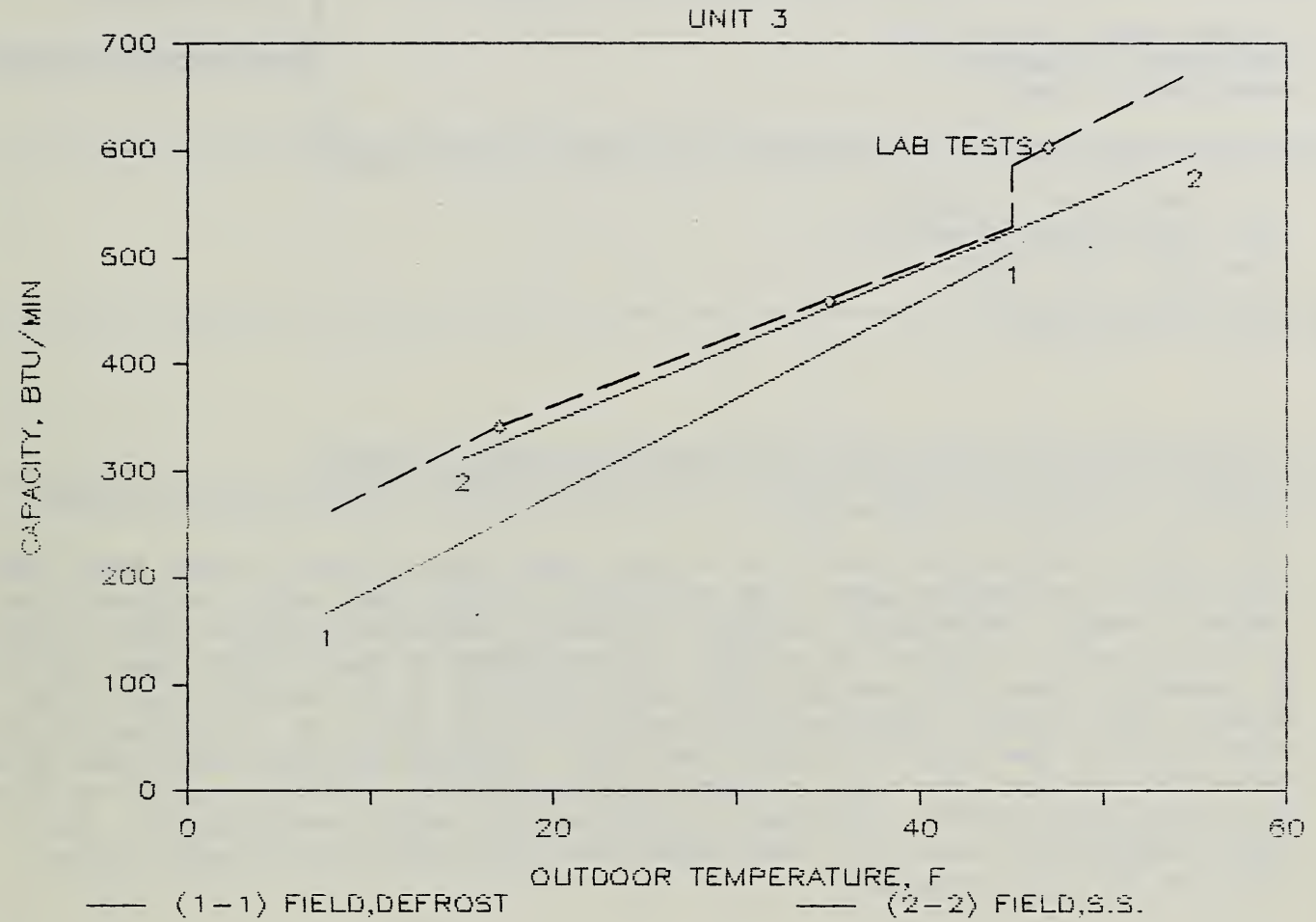

Figure 4.34 Comparison of Laboratory and Field Test Results

NBS-114A (REV. 2-8C)

U.S. DEPT. OF COMM. BIBLIOGRAPHIC DATA SHEET (See instructions)	1. PUBLICATION OR REPORT NO. NBSIR 87-3528	2. Performing Organ. Report No.	3. Publication Date February 1987

4. TITLE AND SUBTITLE

FIELD PERFORMANCE OF THREE RESIDENTIAL HEAT PUMPS IN THE HEATING MODE

5. AUTHOR(S)

James Y. Kao, William J. Mulroy, and David A. Didion

6. PERFORMING ORGANIZATION (If joint or other than NBS, see instructions)

NATIONAL BUREAU OF STANDARDS
DEPARTMENT OF COMMERCE
WASHINGTON, D.C. 20234

7. Contract/Grant No.

8. Type of Report & Period Covere

9. SPONSORING ORGANIZATION NAME AND COMPLETE ADDRESS (Street, City, State, ZIP)

U. S. Department of Energy
1000 Independence Avenue, SW
Washington, DC 20585

10. SUPPLEMENTARY NOTES

☐ Document describes a computer program; SF-185, FIPS Software Summary, is attached.

11. ABSTRACT (A 200-word or less factual summary of most significant information. If document includes a significant bibliography or literature survey, mention it here)

This report presents the results of a field performance study of three heat pumps operating in the heating mode. The objective of this study was to evaluate the thermal, energy, defrosting, cycling, and other related performance under in-situ conditions and to confirm the validity of Department of Energy (DoE) test procedures by comparing these field results with those obtained in the laboratories. The seasonal COPs without auxiliary heat were 1.83, 2.31, and 1.92. The seasonal COPs with auxiliary heat were 1.71, 1.95, and 1.60. General agreement was found in two houses for cycling rates and building load estimation. Defrost penalty was found to be light above 40°F. One house was analyzed for cyclic performances. The cyclic degradation factor (C_D) was found to be worse than the optional factor (0.25) of the DoE procedure.

12. KEY WORDS (Six to twelve entries; alphabetical order; capitalize only proper names; and separate key words by semicolons)

defrosting; field performance; field performance of heat pumps; heat pumps; heat pump test methods; heating seasonal performance

13. AVAILABILITY

☒ Unlimited
☐ For Official Distribution. Do Not Release to NTIS
☐ Order From Superintendent of Documents, U.S. Government Printing Office, Washington, D.C. 20402.
☒ Order From National Technical Information Service (NTIS), Springfield, VA. 22161

14. NO. OF PRINTED PAGES 79

15. Price $13.95

USCOMM-DC 6043-P8